AD _____

# WATER-REPELLENT TREATMENTS
# ON BATTLE DRESS UNIFORM FABRIC

by
**Phillip Gibson**

September 2005

Final Report
October 2003 – October 2004

# REPORT DOCUMENTATION PAGE

*Form Approved*
*OMB No. 0704-0188*

Public reporting burden for this collection of information is estimated to average 1 hour per response, including the time for reviewing instructions, searching existing data sources, gathering and maintaining the data needed, and completing and reviewing this collection of information. Send comments regarding this burden estimate or any other aspect of this collection of information, including suggestions for reducing this burden to Department of Defense, Washington Headquarters Services, Directorate for Information Operations and Reports (0704-0188), 1215 Jefferson Davis Highway, Suite 1204, Arlington, VA 22202-4302. Respondents should be aware that notwithstanding any other provision of law, no person shall be subject to any penalty for failing to comply with a collection of information if it does not display a currently valid OMB control number. **PLEASE DO NOT RETURN YOUR FORM TO THE ABOVE ADDRESS.**

| 1. REPORT DATE *(DD-MM-YYYY)*<br>29 - 09 - 2005 | 2. REPORT TYPE<br>Final | 3. DATES COVERED *(From - To)*<br>October 2003 – October 2004 |
|---|---|---|

| 4. TITLE AND SUBTITLE<br><br>WATER-REPELLENT TREATMENTS ON BATTLE DRESS UNIFORM FABRIC | 5a. CONTRACT NUMBER |
|---|---|
| | 5b. GRANT NUMBER |
| | 5c. PROGRAM ELEMENT NUMBER<br>0602786A |

| 6. AUTHOR(S)<br><br>Phillip Gibson | 5d. PROJECT NUMBER |
|---|---|
| | 5e. TASK NUMBER |
| | 5f. WORK UNIT NUMBER |

| 7. PERFORMING ORGANIZATION NAME(S) AND ADDRESS(ES)<br>U.S. Army Research, Development and Engineering Command<br>Soldier Systems Center<br>Macromolecular Science Team<br>ATTN: AMSRD-NSC-SS-MS<br>Natick, MA 01760-5020 | 8. PERFORMING ORGANIZATION REPORT NUMBER<br><br>NATICK/TR-05/023 |
|---|---|

| 9. SPONSORING / MONITORING AGENCY NAME(S) AND ADDRESS(ES) | 10. SPONSOR/MONITOR'S ACRONYM(S) |
|---|---|
| | 11. SPONSOR/MONITOR'S REPORT NUMBER(S) |

**12. DISTRIBUTION / AVAILABILITY STATEMENT**

Approved for public release; distribution is unlimited.

**13. SUPPLEMENTARY NOTES**

**14. ABSTRACT**

This report documents testing carried out on several water-repellent treatments for fabrics based on nanotechnology approaches. The intent was to compare the effectiveness and durability of durable water repellent (DWR) fabric treatments for applications such as military uniforms. Various performance properties such as hydrostatic head (resistance to liquid water penetration), liquid spray repellency, fabric breathability/air permeability, and fabric pore size were measured before and after laundering.

**15. SUBJECT TERMS**

| | | | | | |
|---|---|---|---|---|---|
| FIBERS | CLOTHING | RESISTANCE | PENETRATION | AIR PERMEABILITY | PROTECTIVE TREATMENTS |
| FABRICS | DIFFUSION | PROTECTION | PERMEABILITY | WATER REPELLENTS | BDU(BATTLE DRESS UNIFORM) |
| LAUNDER | UNIFORMS | DURABILITY | BREATHABILITY | NANOTECHNOLOGY | |
| COMFORT | PORE SIZES | REPELLENTS | WATERPROOFING | LIQUID PENETRATION | |

| 16. SECURITY CLASSIFICATION OF: | | | 17. LIMITATION OF ABSTRACT | 18. NUMBER OF PAGES | 19a. NAME OF RESPONSIBLE PERSON<br>Phillip W. Gibson |
|---|---|---|---|---|---|
| a. REPORT<br>UNCLASSIFIED | b. ABSTRACT<br>UNCLASSIFIED | c. THIS PAGE<br>UNCLASSIFIED | UU | 66 | 19b. TELEPHONE NUMBER *(include area code)*<br>508-233-4273 |

**Standard Form 298 (Rev. 8-98)**
**Prescribed by ANSI Std. Z39.18**

# Table of Contents

**This page intentionally left blank**

# List of Figures

## Preface


This report documents testing carried out on several water-repellent fabric treatments for an informal ad-hoc project "Near-Term Water-Repellent Nanotechnology Demonstration," during the period October 2003 – October 2004.  The results contained in this report were produced by the Supporting Sciences and Technology Directorate (SS&TD) in support of a larger effort by the Natick Soldier Center to evaluate the effectiveness of some of these treatments.  The work was funded under Program Element 0602786A.

# WATER-REPELLENT TREATMENTS ON BATTLE DRESS UNIFORM FABRIC

## 1. Introduction

This report documents testing carried out on several water-repellent treatments—based on nanotechnology approaches—for fabrics used in the production of Battle Dress Uniforms (BDUs). The intent was to compare the effectiveness and durability of durable water repellent (DWR) fabric treatments for applications such as military uniforms. Various performance properties such as hydrostatic head (resistance to liquid water penetration), liquid spray repellency, fabric breathability/air permeability, and fabric pore size were measured before and after laundering.

The purpose of this testing with regards to the water-repellent treatments was to ensure that the treatment didn't impact the breathability or air permeability of the fabric. Many durable water-repellent (DWR) treatments, if applied too heavily, can close off the fabric pores and reduce vapor diffusion or convective flow through the fabric.

Two of the water-repellent treatments had good durability to laundering. One treatment had very poor durability, and lost all its water-repellent properties after 20 laundering cycles. The Quarpel-treated control fabric performed better than any of the experimental treatments. None of the water-repellent treatments significantly affected the breathability, air flow resistance, or pore size of the BDU fabric.

It was found that the standard BDU fabric can be modified with very effective water-repellent treatments. Soldiers' duty and combat uniforms can be made water-resistant and retain the same air permeability and "breathability" properties as the untreated wicking fabric. Several questions arose as a result of this work. What are the physiological implications of changing the BDU fabric from a wicking fabric to a non-wicking fabric? Will the fabric still be comfortable when a soldier is sweating heavily? Will liquid sweat now remain on the skin underneath the fabric, and is this bad or good?

Following a separate field trial using combat uniforms with and without a DWR treatment, it was found that these treatments decreased the comfort of the uniform in hot environments. The differences between the comfort of the Control uniform and those treated with the DWR treatments are probably not due to intrinsic differences in the air permeability or the water vapor diffusion resistance (breathability) of the fabric. It is more likely that the non-wicking behavior of the fabric was responsible for perceived comfort differences, per comments from the field trial, and by analysis of wicking/comfort properties contained in this report.

Note: The results contained in this report were produced by the Supporting Sciences and Technology Directorate (SS&TD) in support of a larger effort by the Natick Soldier Center to evaluate the effectiveness of some of these treatments. This report only documents those tests and analyses carried out by SS&TD.

## 2. Test Materials

Three different fabric treatments based on nanotechnology were selected for application to the Battle Dress Uniform (BDU) fabric. To protect proprietary information, the treatments and companies supplying the treatments are not identified, but are given as the "Red," "Blue," and "Green" treatments.

The treatments were applied to the BDU fabric, which is a 50% nylon / 50% cotton blend fabric used in the army combat uniform. The BDU fabric is not normally treated with a water-repellent finish. However, an older version of the U.S. Army's chemical protective suit (Battle Dress Overgarment or BDO) did use the BDU fabric treated with an oil and water-repellent finish (Quarpel treatment). This BDO fabric was used to compare the effectiveness of the three nanotechnology water-repellent treatments.

### Test Fabrics

1. BDU Fabric (untreated)
2. Battle Dress Overgarment (BDO) shell fabric
   (same as BDU, but with Quarpel water/oil repellent treatment)
3. Green treatment on BDU
4. Blue treatment on BDU
5. Red treatment on BDU

For some of the laboratory tests, a variety of commercial fabrics incorporating various DWR treatments are included to help in the comparison of the performance of the Red, Blue, and Green treatments

### Standard Comparison Fabrics

1. Expanded PTFE (ePTFE) microporous membrane
   Joint Services Lightweight Integrated Suit Technology (JSLIST) shell fabric
   without Quarpel treatment
2. JSLIST Quarpel-treated shell fabric
3. JSLIST shell fabric with Nanotex water repellent treatment
4. Schoeller Dynamic Extreme – stretch woven soft shell fabric with DWR
5. Nextec 1 silicone DWR on woodland camouflage 100% FR cotton
6. Nextec 2 silicone DWR on desert camouflage 100% FR cotton
7. Nextec 3 silicone DWR 100% nylon fabric (Tuckermans style)
8. Nextec 4 silicone DWR 100% nylon fabric (Summit style)

## 3. Laboratory Test Methods and Results

### Hydrostatic Head – Water Entry Pressure

Hydrostatic head is the pressure required to force liquid water through the fabric. The test system is shown in Figure 1. Breakthrough pressure is defined as 3 leakage spots on the fabric.
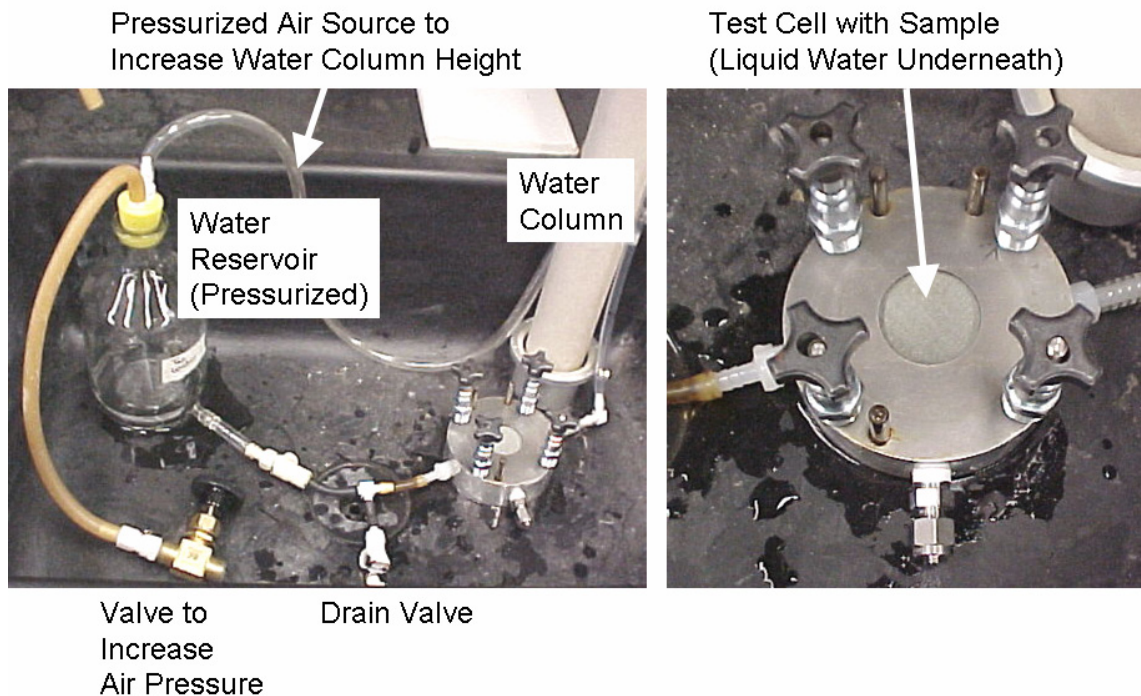


Figure 1.  Hydrostatic head test setup.  Water column height increased until liquid breakthrough occurs.

Figure 2 shows the initial unlaundered hydrostatic head measurements for the test fabrics and comparison treated fabrics. The Red, Blue, and Green treatments are not as water-resistant as many other common DWR treatments.
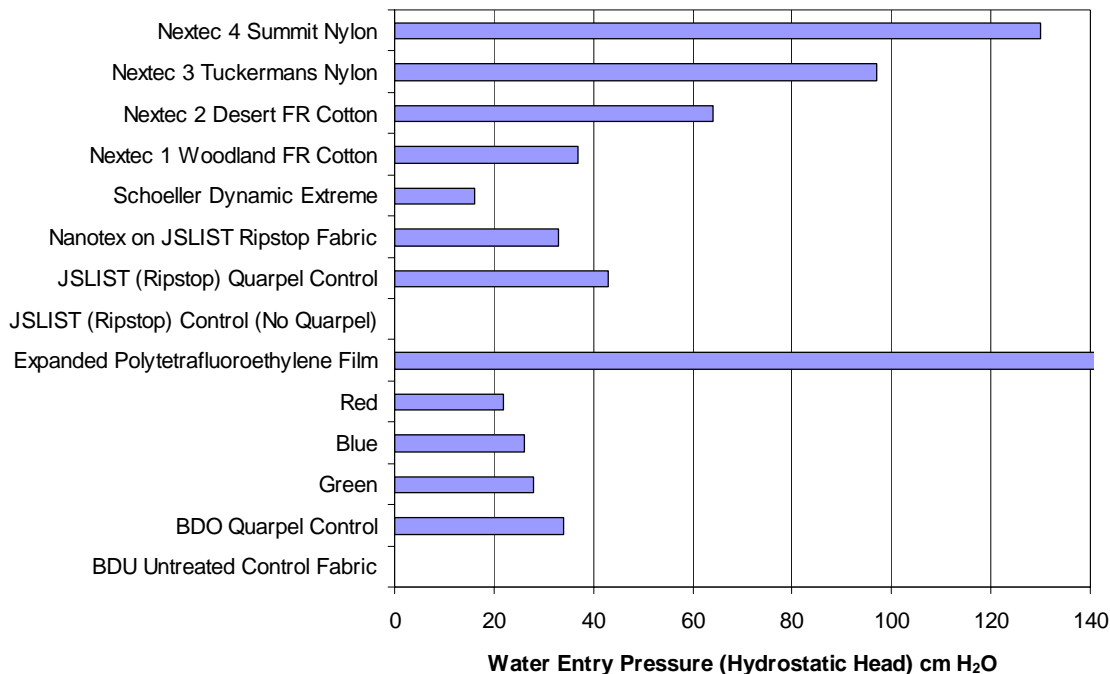


Figure 2. Initial (before laundering) hydrostatic head of four water-repellent fabric treatments compared to other various standard water-repellent treatments.

Hydrostatic head was measured after 5, 10, 15, and 20 laundering cycles, as shown in Figure 3.
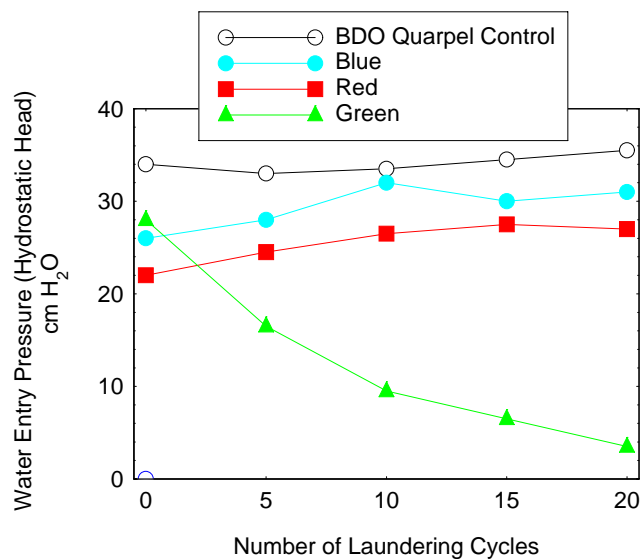


Figure 3. Hydrostatic head of four water-repellent fabric treatments after laundering. Fabric shrinkage after laundering can increase hydrostatic head due to smaller fabric pores.

4

Pictures were taken of the unlaundered and 5-cycle laundered samples to show the typical liquid breakthrough patterns, and are seen in Figs. 4 - 6. The Blue, Green, and Red treatments are nearly as good as Quarpel, but are not as effective as the silicone durable water repellent (DWR) coating (Nextec, EPIC, Encapsil).

**Unlaundered – Four Water-Repellent Treatments**

BDU Untreated Control Fabric
Sample wetted out,
no hydrostatic head

BDO Quarpel Control
Breakthrough Pressure
35 and 33 cm H20
34 cm average
13.4 inches H20
0.48 psi
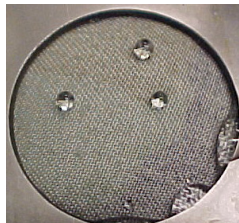


Green
Breakthrough Pressure
28 and 27 cm H20
28 cm average
11 inches H20
0.40 psi
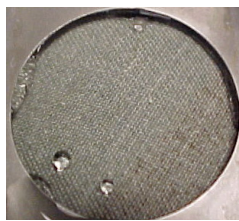


Blue
Breakthrough Pressure
26 and 26 cm H20
26 cm average
10 inches H20
0.37 psi
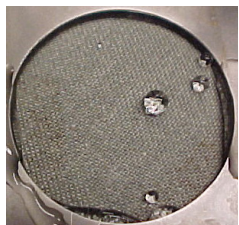


Red
Breakthrough Pressure
24 and 20 cm H20
22 cm average
8.7 inches H20
0.31 psi
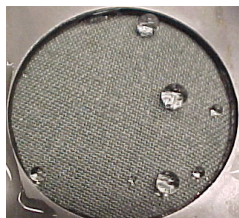


Figure 4. Hydrostatic head breakthrough pressure of four water-repellent treatments.

**Unlaundered Comparison Standard Control Fabrics**

Expanded Polytetrafluoroethylene Film
Breakthrough Pressure (no breakthrough)
>> 150 cm H20
>> 60 inches H20. >> 2.1 psi
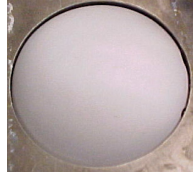
JSLIST (Ripstop) Quarpel Control
Breakthrough Pressure
43 cm H20 average
16.9 inches H20, 0.61 psi
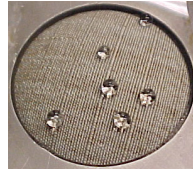
Nanotex on JSLIST Ripstop Fabric
Breakthrough Pressure
33 cm H20 average
13 inches H20, 0.47 psi
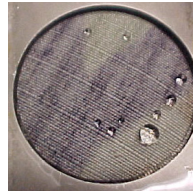
Schoeller Dynamic Extreme
Breakthrough Pressure
16 cm H20 average
6.3 inches H20, 0.23 psi
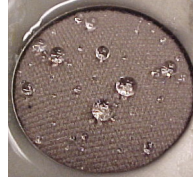
Nextec 1 Woodland FR Cotton
Breakthrough Pressure
37 cm H20 average
14.6 inches H20, 0.52 psi
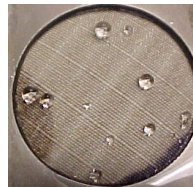
Nextec 2 Desert FR Cotton
Breakthrough Pressure
64 cm H20 average
25.2 inches H20, 0.91 psi

Nextec 3 Tuckermans Nylon
Breakthrough Pressure
97 cm H20 average
38.2 inches H20,1.4 psi
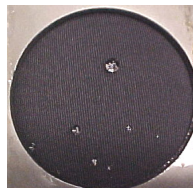
Nextec 4 Summit Nylon
Breakthrough Pressure
130 cm H20 average
51 inches H20, 1.8 psi
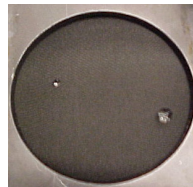
Figure 5. Hydrostatic head breakthrough pressure of unlaundered comparison fabrics.

## 5 Laundering Cycles – Four Water-Repellent Treatments

BDO Quarpel Control
Breakthrough Pressure
32 and 34 cm H20
33 cm average
13.0 inches H20
0.47 psi
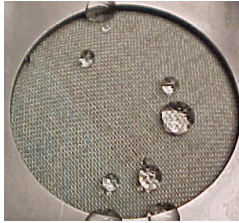
Green
Breakthrough Pressure
18 and 15 cm H20
16.5 cm average
6.5 inches H20
0.23 psi
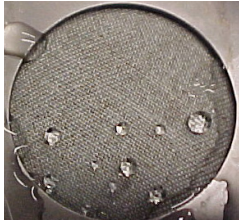
Blue
Breakthrough Pressure
27 and 29 cm H20
28 cm average
11 inches H20
0.40 psi
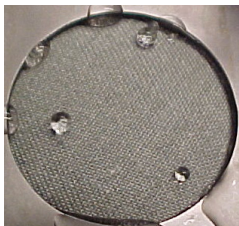
Red
Breakthrough Pressure
24 and 25 cm H20
24.5 cm average
9.6 inches H20
0.35 psi
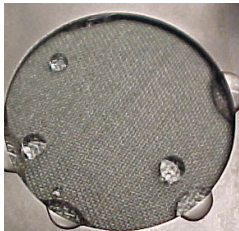
Figure 6.  Hydrostatic head breakthrough pressure of four water-repellent treatment after five laundering cycles.

**Spray Rating (Water Repellency)**

Fabrics held at a 25-degree angle were sprayed with water, and pictures were taken to qualitatively determine the effectiveness of the water-repellent coating.  This is a lower angle than standard testing and allows a better view of real-world effects important for liquid-repellent coatings.  Materials that allowed liquid to soak into the fabric, or that allow many large drops to be retained on the surface have degraded repellency.  Materials that have only a few small liquid drops have maintained their water repellency.

Comparison spray on Initial BDU Control (water immediately soaked into the fabric).



| Number of Laundering Cycles | BDO Quarpel Control | Green | Blue | Red |
|---|---|---|---|---|
| Initial | | | | |
| 5 | | | | |
| 10 | | | | |
| 15 | | | | |
| 20 | | | | |
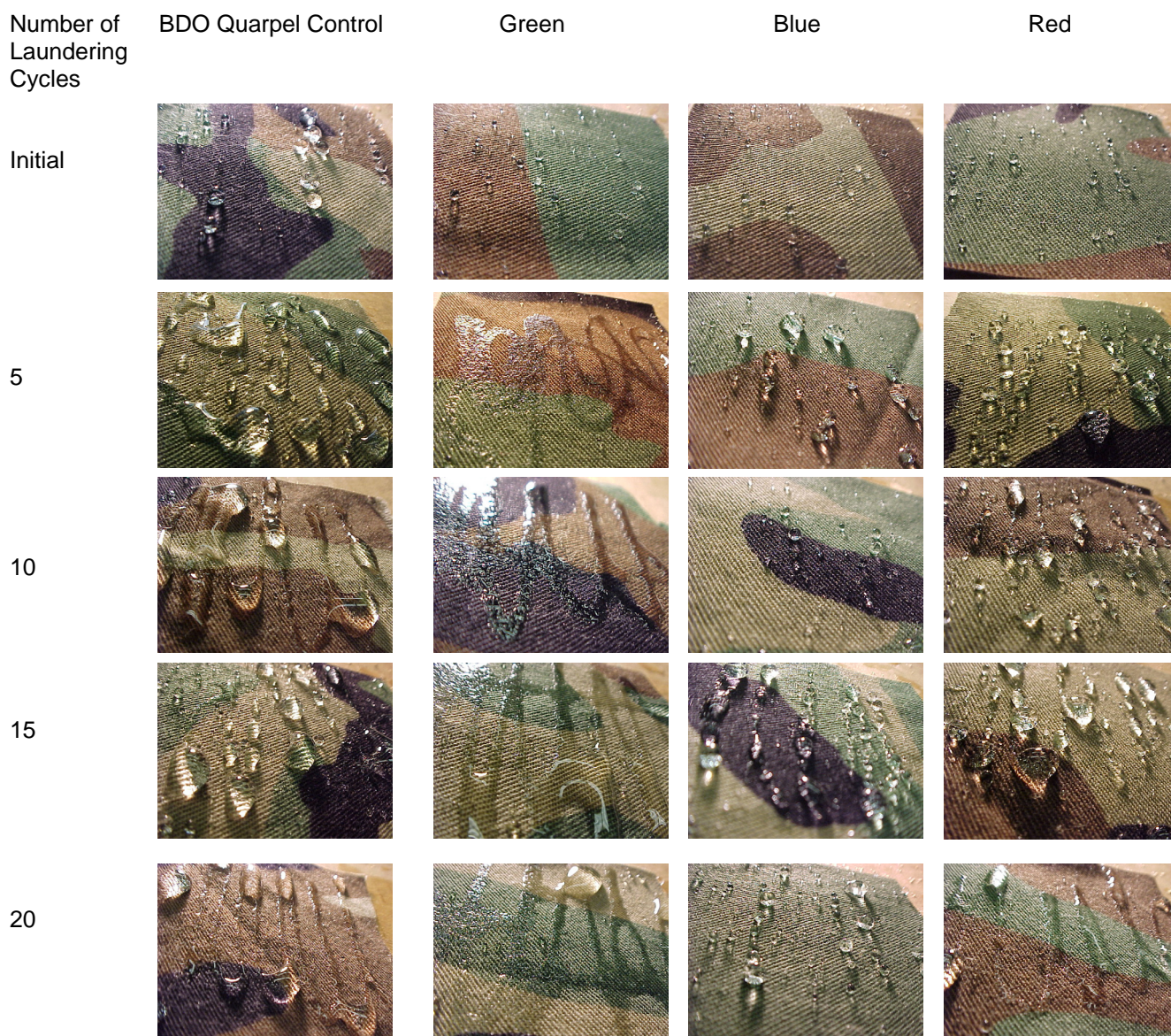


Figure 7.  Water spray repellency of four fabric treatments affected by laundering.

**Spray Rating -- Unlaundered Comparison Standard Control Fabrics**

Expanded
PTFE Film
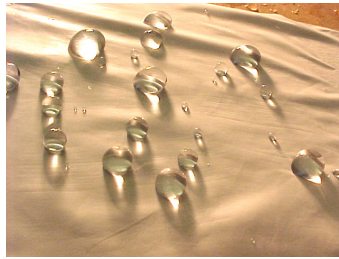
JSLIST
(Ripstop)
Control
(no Quarpel)

JSLIST
(Ripstop)
Quarpel
Control
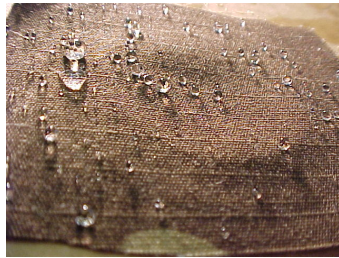
Nanotex on
JSLIST
Ripstop
Fabric
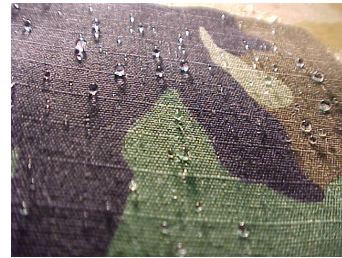
Schoeller
Dynamic
Extreme

Nextec 1
Woodland
FR Cotton
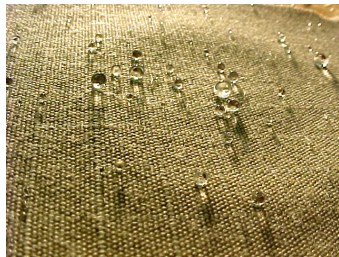
Nextec 2
Desert
FR Cotton

Nextec 3
Tuckermans
Nylon
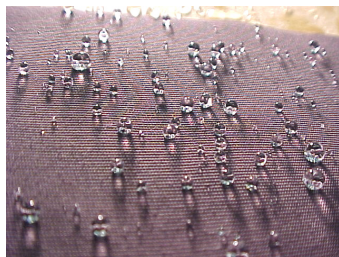
Nextec 4
Summit
Nylon
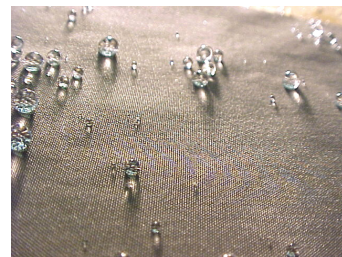
Figure 8. Water spray repellency of unlaundered comparison fabrics.

**Mean Pore Size - Capillary Liquid Expulsion Porometry**

Pore size measurements were made with the Model CFP1500AEX automated capillary flow porometer manufactured by Porous Materials, Inc.  Pore sizes were measured by saturating the porous material with a wetting liquid of known surface tension.  Gas pressure on one side of the sample was increased until liquid from the largest pores was expelled.  As the pressure increased, smaller pores opened up and the flow rate of gas through the sample increased until all the accessible pores were emptied.  A plot of the pressure versus flow rate through the wetted sample, when compared with the equivalent pressure/flow rate curve for a dry sample, gave an estimate of pore size distribution in the material.  In the standard mode, the pores measured with this method only include those pores that provide a continuous path from one side of the material to the other; dead-end pores are not measured with this method.  The wetting liquid used for our pore size measurements was Galden perfluorinated liquid HT 230, with a surface tension of 19 dynes/cm, and a low vapor pressure.  Liquids of low surface tension allow lower pressures to be used in the porometry experiment, while low vapor pressures minimize liquid evaporation during a test.

Sample data from a typical porometry test is shown below for an electrospun polyurethane membrane.
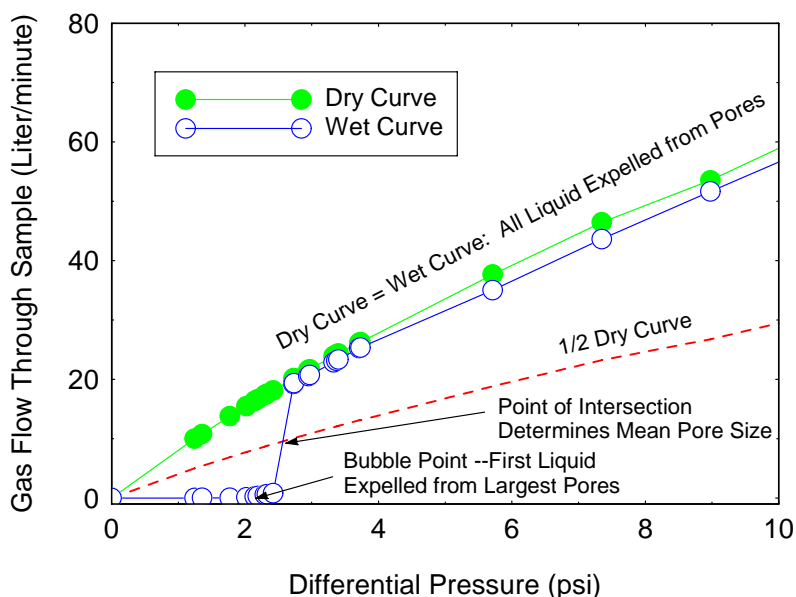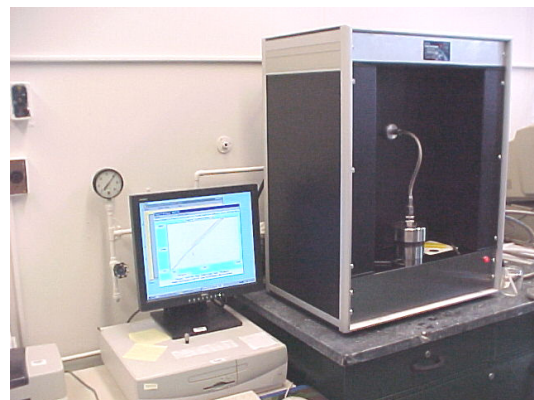


(a)                                                        (b)

Figure 9.  (a) Example capillary expulsion porometry for electrospun Pellethane membrane;       (b) PMI Porometer.

The measured mean pore sizes for the fabrics are shown below.
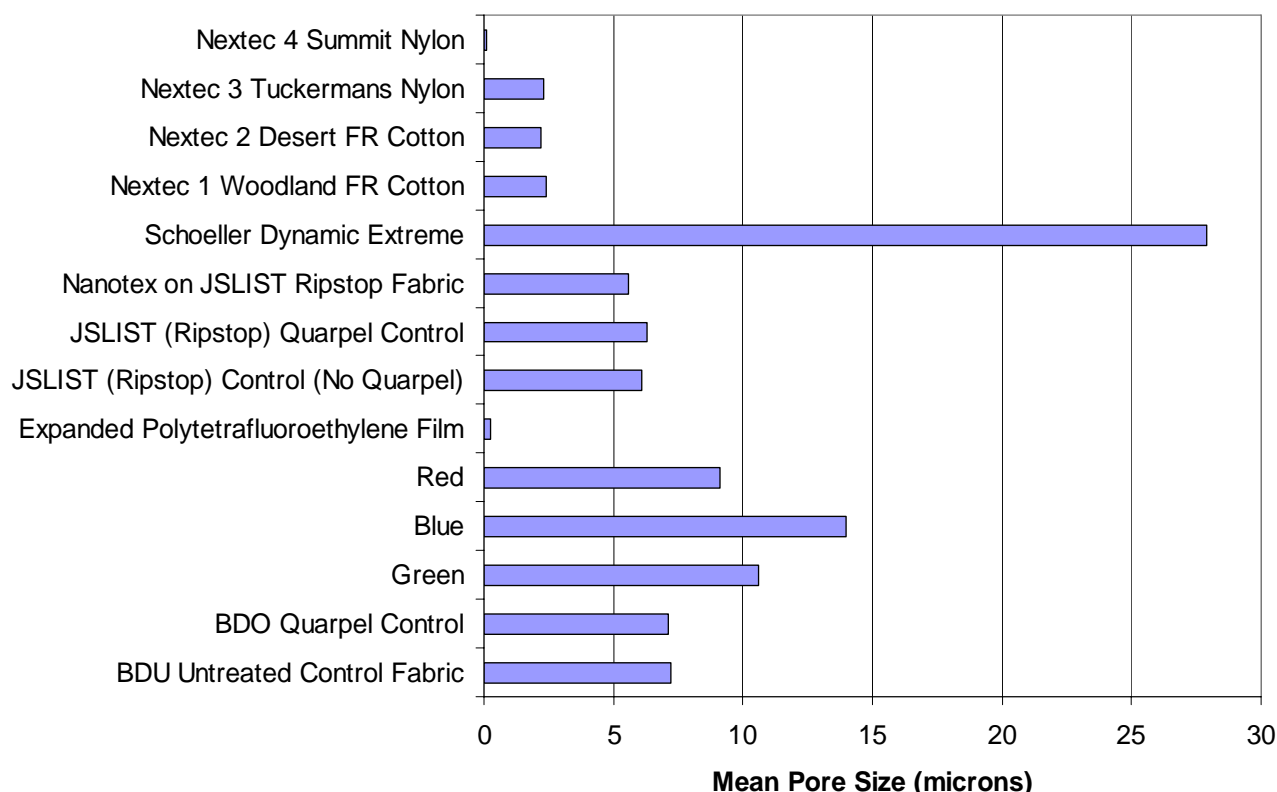


Figure 10. Mean pore sizes.

The fabric treatments didn't significantly affect the mean pore size of the base fabric. The variation in pore size between the Red, Blue, and Green treatments is similar to the pore sizes of the other base fabrics such as the JSLIST controls. The slightly larger pore sizes of the "Blue" fabric did not affect transport properties such as air permeability or water vapor diffusion (breathability), as shown in the next section.

**Water Vapor Diffusion (Breathability) and Air Flow Resistance (Air Permeability): Dynamic Moisture Permeation Cell**

Fabrics were tested for water vapor diffusion (breathability), and air flow resistance (air permeability) with the Dynamic Moisture Permeation Cell (DMPC). Sample area was 10 cm$^2$, and test temperature was 30°C. Three samples of each material were tested. A summary of the test method for measuring these properties is given in Appendix A. Further information is in the literature cited in References 1-5. Three samples of each of the laundered fabrics were also tested, but aren't shown, since it is the initial unlaundered values that are of most interest.

The purpose of this testing with regards to the water-repellent treatments was to ensure that the treatment doesn't impact the breathability or air permeability of the fabric. Many durable water repellent (DWR) treatments, if applied too heavily, can close off the fabric pores and reduce vapor diffusion or convective flow through the fabric. The Nextec silicone encapsulation treatment is a good example of this. Although the Nextec coating provides good water-resistant fabrics, it can also severely impact the breathability of fabrics if the coating is too heavy.

**Air Permeability and Air Flow Resistance**

Figure 11 shows the measured air flow resistance, which is the inverse of air permeability. Low values of air flow resistance correspond to high air permeability. The small differences seen between the Red, Green, Blue, and Quarpel control fabrics aren't very significant.
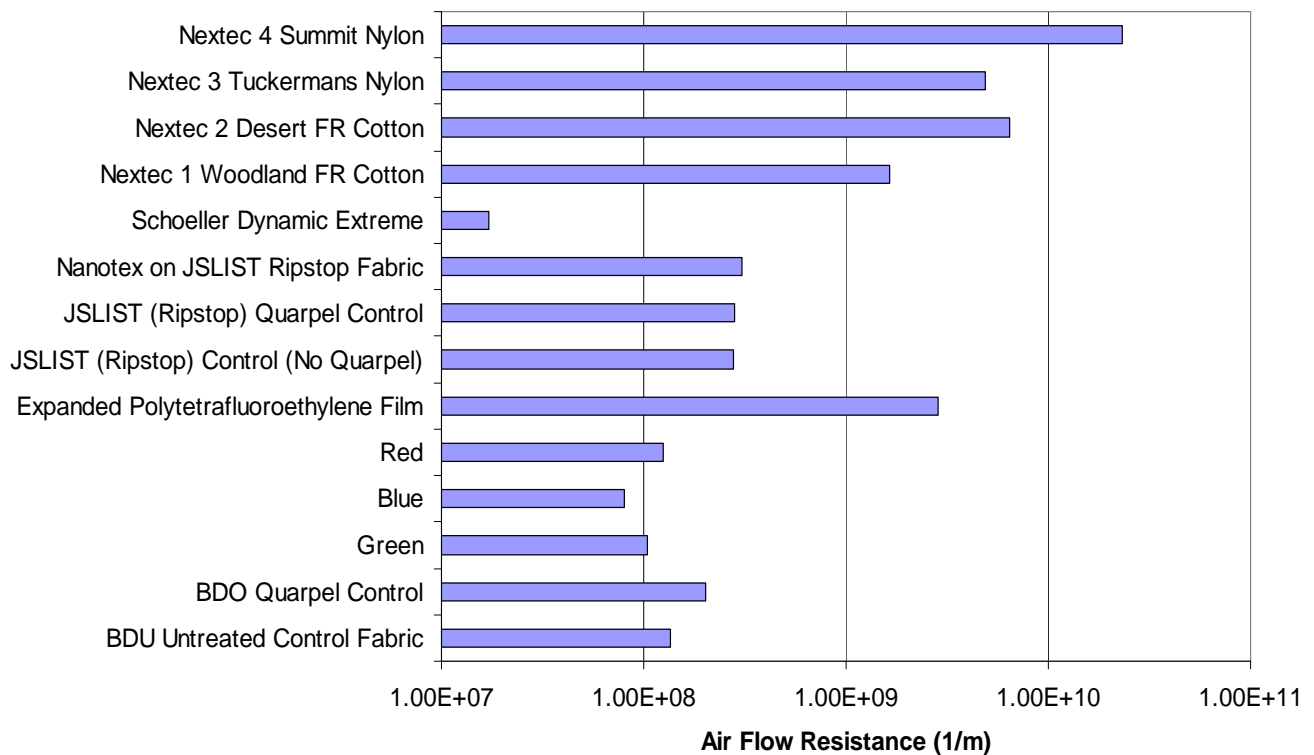
Figure 11. Air flow resistance.

## Water Vapor Diffusion Resistance and Water Vapor Flux

Figure 12 shows the water vapor diffusion resistance of the samples. The higher the resistance, the less water vapor is able to get through. For this particular set of test conditions, any value above about 2000 s/m means that the material is essentially impermeable to water vapor. The expanded polytetrafluorethylene (ePTFE) film is extremely breathable, and serves as a practical lower limit on resistance.
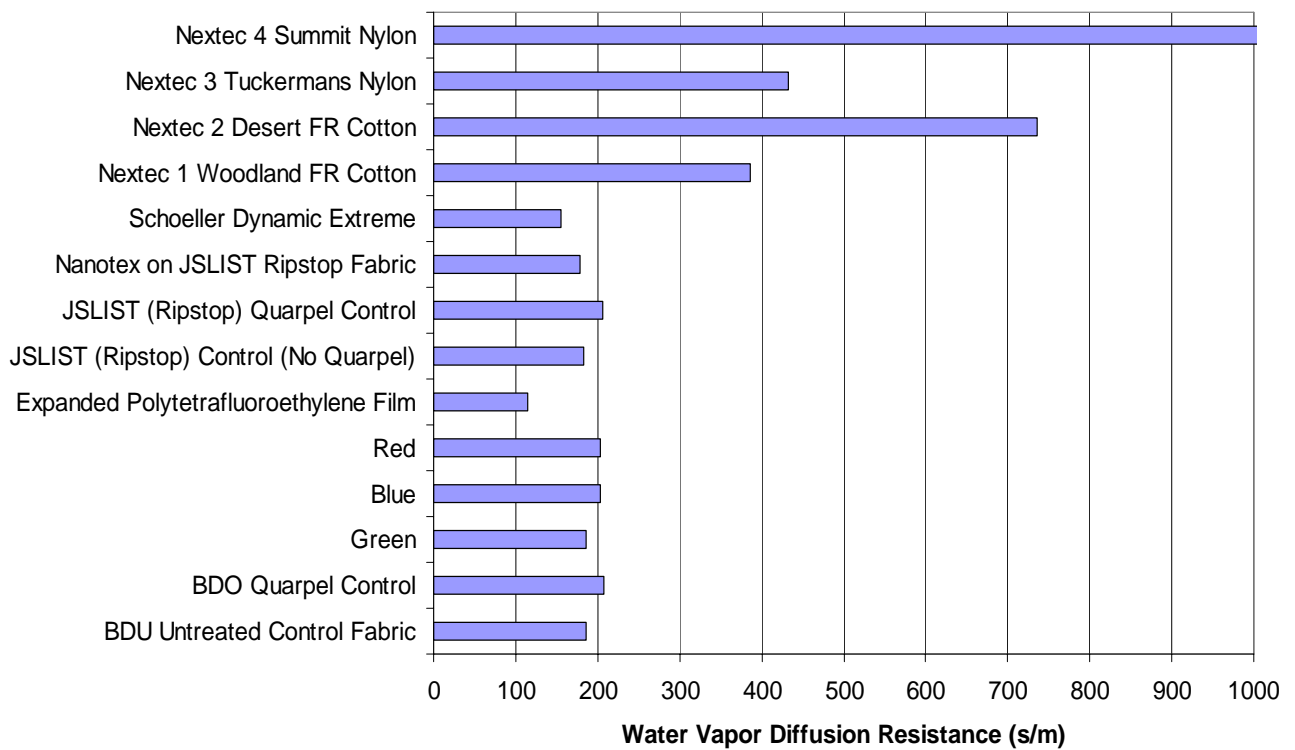


Figure 12. Water vapor diffusion resistance. No significant differences between the Red, Blue, and Green water-repellent treatments.

14
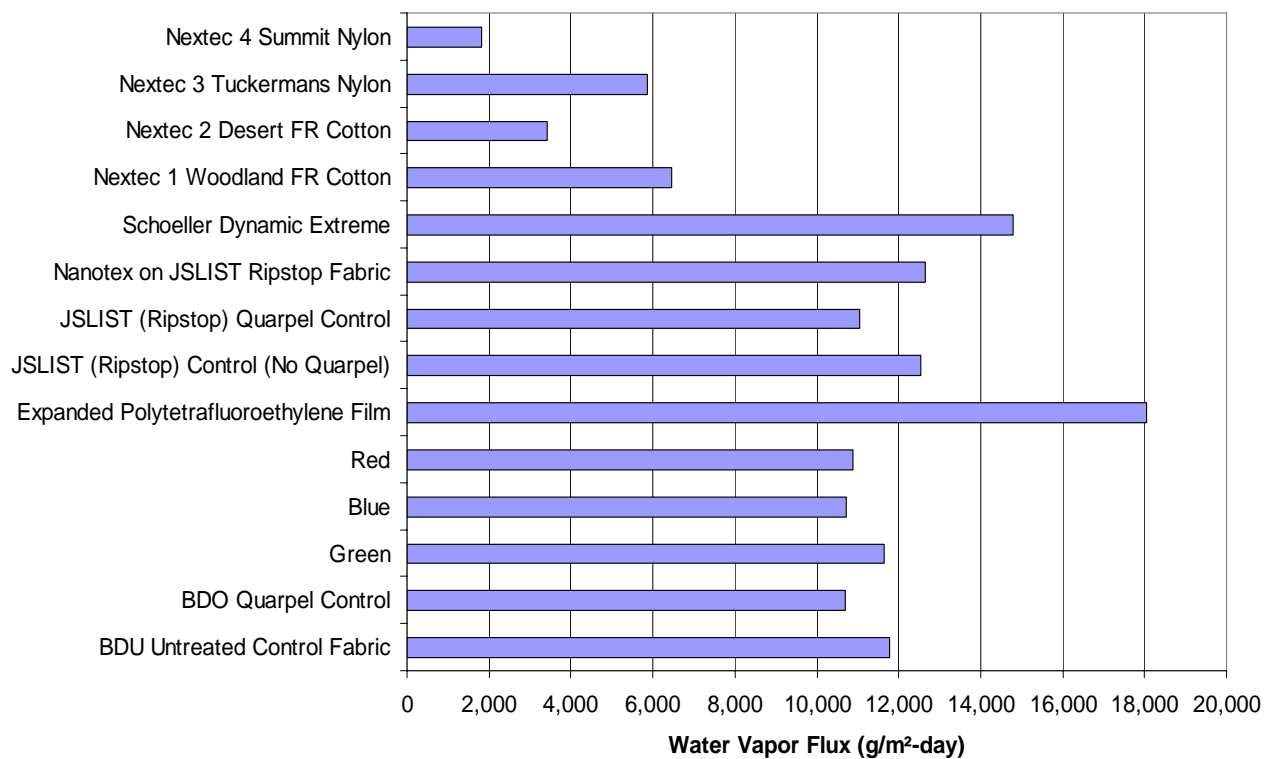


Figure 13.  Water vapor flux. No significant differences between the Red, Blue, and Green water-repellent treatments.

14

## 4. Testing of Uniforms After Field Trial

**Water Vapor Diffusion (Breathability) and Air Flow Resistance (Air Permeability)**

Following the laboratory tests given in the previous sections of this report, the two better-performing nanotechnology-based DWR treatments were chosen for a field trial. Treatments were applied to the Close Combat Uniform (CCU) fabric, and used in a warm-weather field trial at the Joint Readiness Test Center (JRTC) in Fort Polk, Louisiana. Following the field trial, the uniforms were tested to determine any change in fabric properties due to the treatment (the treated uniforms were found to be uncomfortable in a hot/wet environment). The treatments are now identified as "Nanotex" and "DuPont."

The Close Combat Uniforms (CCU) from the field trial at JRTC were tested for water vapor diffusion (breathability), and air flow resistance (air permeability). Sample area was 10 cm$^2$, and test temperature was 30°C (test method in Appendix A). One area of each uniform was tested. Samples were not cut from the uniforms; the test cell was clamped onto a single layer fabric region of the uniform (bottom of blouse or top of pants) and tested directly.

The materials were:

Control CCU-HWBDU:
Control Hot Weather Battle Dress Uniform (HWBDU) fabric (nylon/cotton ripstop)

DuPont CCU-HWBDU:
DuPont Durable Water Repellent (DWR) treatment on HWBDU (no field wear)

DuPont CCU-HWBDU, Worn/Laundered:
DuPont DWR on HWBDU after being worn and laundered

Nanotex CCU-HWBDU:
Nanotex Durable Water Repellent (DWR) treatment on HWBDU (no field wear)

Nanotex CCU-HWBDU, Worn/Laundered:
Nanotex DWR on HWBDU after being worn and laundered

The purpose of this testing with regards to the water-repellent treatments is to ensure that the treatment doesn't impact the breathability or air permeability of the fabric. Many durable water repellent (DWR) treatments, if applied too heavily, can close off the fabric pores and reduce vapor diffusion or convective flow through the fabric. The commercially available Nextec En-cap-sil silicone encapsulation fabric treatment is a good example of this. Although the Nextec coating provides good water-resistant fabrics, it can also severely impact the breathability of fabrics if the coating is too heavy.

## Air Permeability and Air Flow Resistance

Figure 14 shows the measured air flow resistance, which is the inverse of air permeability. Low values of air flow resistance correspond to high air permeability. The small differences seen between the various uniform fabrics aren't very significant. The control fabric is slightly more air permeable (lower flow resistance), but the difference isn't enough to explain the large reported differences in comfort between the control and the treated fabrics.
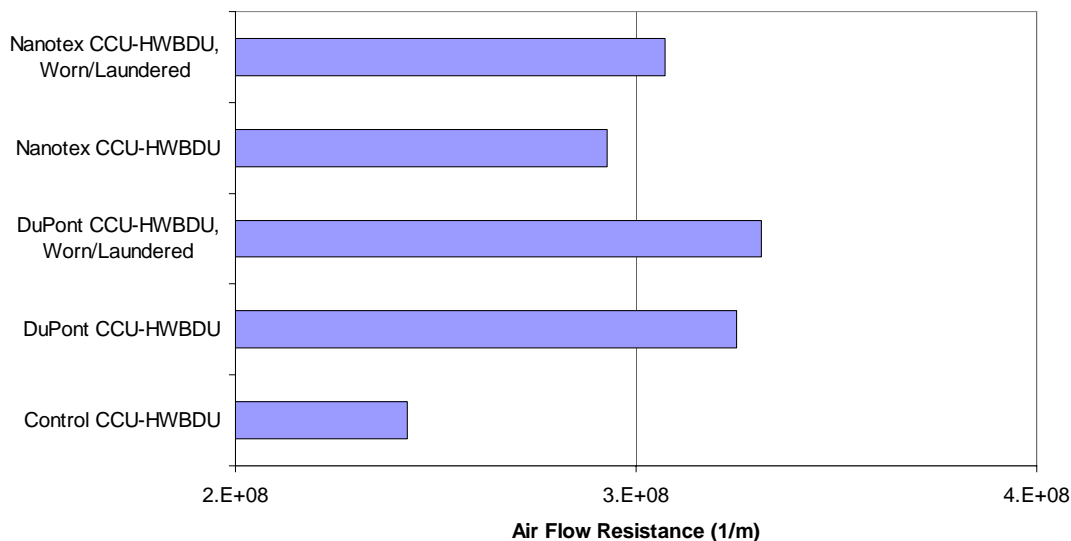


Figure 14. Air flow resistance.

## Water Vapor Diffusion Resistance and Water Vapor Flux

Figure 15 shows the water vapor diffusion resistance of the samples. The higher the resistance, the less water vapor is able to get through.
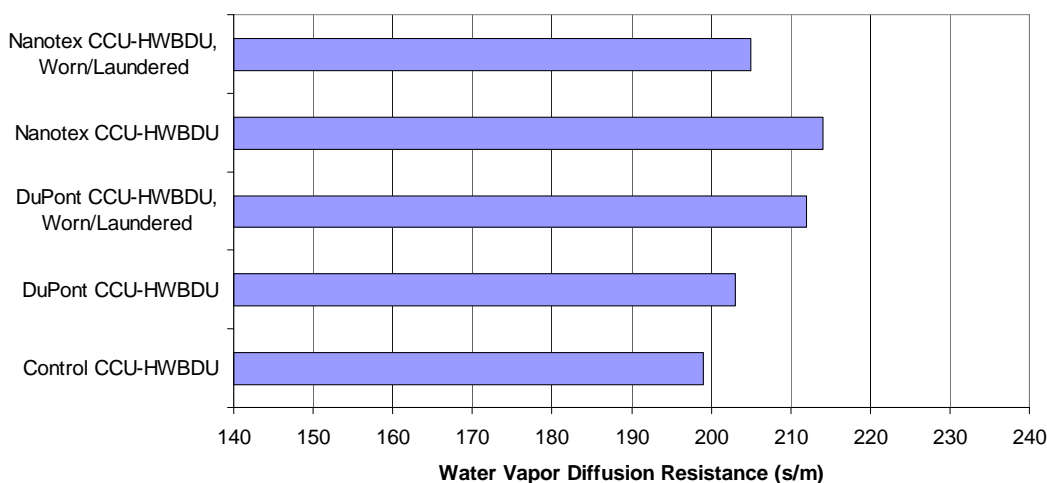


Figure 15. Water vapor diffusion resistance. Slight differences between the Control and the DuPont or Nanotex water-repellent treatments.
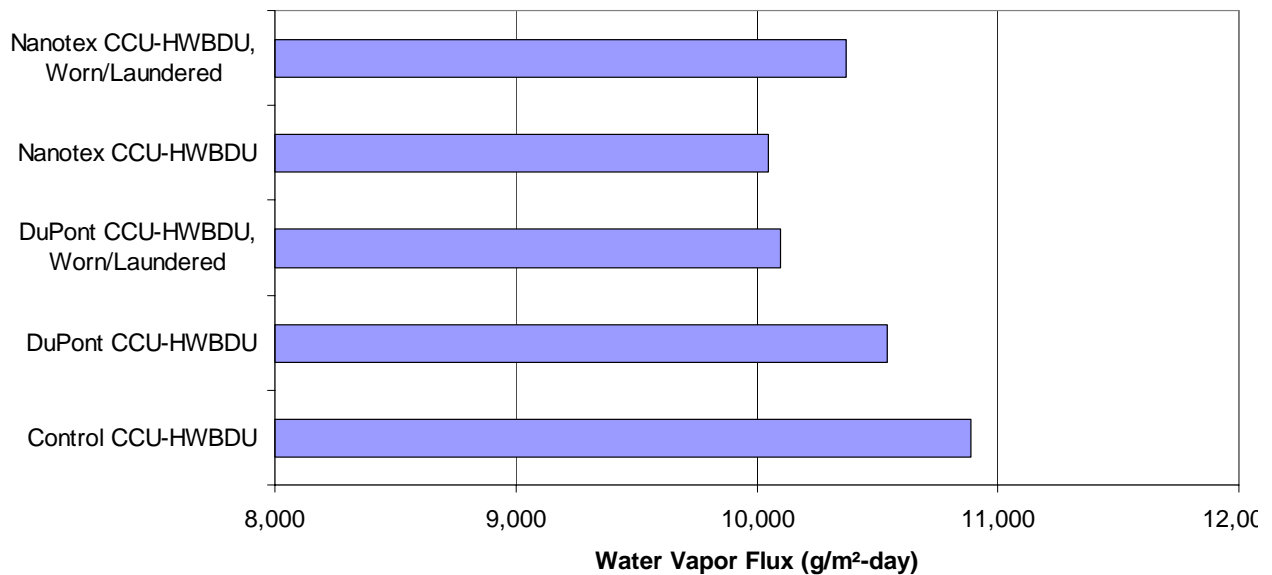
Figure 16. Water vapor flux. Slight differences between the Control, DuPont, or Nanotex water-repellent treatments.

The differences between the comfort of the Control CCU and those treated with the DuPont and Nanotex DWR are probably not due to intrinsic differences in the air permeability or the water vapor diffusion resistance (breathability) of the fabric. It is more likely that the non-wicking behavior of the fabric is responsible for perceived comfort differences, per comments from the field trial. The implications of the wicking versus the nonwicking fabric characteristics are addressed in the next section

## 5.  Water-Repellent Treatment on BDU Fabric:  Physiological/Comfort Implications

The Battle Dress Uniform (BDU) fabric can be modified with very effective water-repellent treatments.  Soldiers' duty and combat uniforms will be water-resistant, but retain the same air permeability and "breathability" properties as the untreated wicking fabric.  What are the physiological implications of changing the BDU fabric from a wicking fabric to a non-wicking fabric?  Will the fabric still be comfortable when a soldier is sweating heavily?  Will liquid sweat now remain on the skin underneath the fabric, and is this bad or good?


### Modeling

The case of a wicking versus a nonwicking fabric, using the BDU fabric as the test case, was examined previously [6,7], and the results are contained in the attached journal article in Appendix B of this report.

A physiological model of an exercising human was combined with a fabric model that accounts for heat transfer, sorption, diffusion, and liquid water transport through the fabric structure.  The physiological model was based on research done for NASA by Stolwijk and Hardy (details in the attached article).

For the wicking fabric (untreated BDU fabric), the modeling approach assumed a very high liquid permeability and very high capillary pressures, which cause any liquid sweat at the skin surface to be quickly distributed within the free porosity of the fabric. This allows us to look at two different clothing materials which are identical in all their properties except that one material will wick sweat away from the skin surface, while the other does not allow wicking through its structure. For the nonwicking case, the liquid sweat remains on the skin, but it is allowed to evaporate based on the local skin temperature, vapor pressure, and local relative humidity gradient.

For the wicking fabric, when liquid sweat is present, wicking effects quickly overwhelm any of the other transport properties (such as diffusion), due to the evaporation of liquid water within the clothing, and the increase in thermal conductivity of the porous textile matrix due to the liquid water that builds up within the clothing layers. An example is shown in Figure 17 for the case of a wicking versus a nonwicking fabric, when a human goes from a light work rate (20 Watt/m$^2$) to a heavy work rate (200 Watt/m$^2$) for 1 hour, and then back to a light work rate. Environmental conditions in both cases are air temperature of 30°C and relative humidity of 65%.  Details of the modeling approach are given in references 6 and 7, and in the attached journal article.

The fabric properties are based on the 50/50 nylon/cotton temperate BDU fabric (twill weave, 0.255 kg/m$^2$ areal density, 550 kg/m$^3$ bulk density, 4.6 x 10$^{-4}$ m thickness).
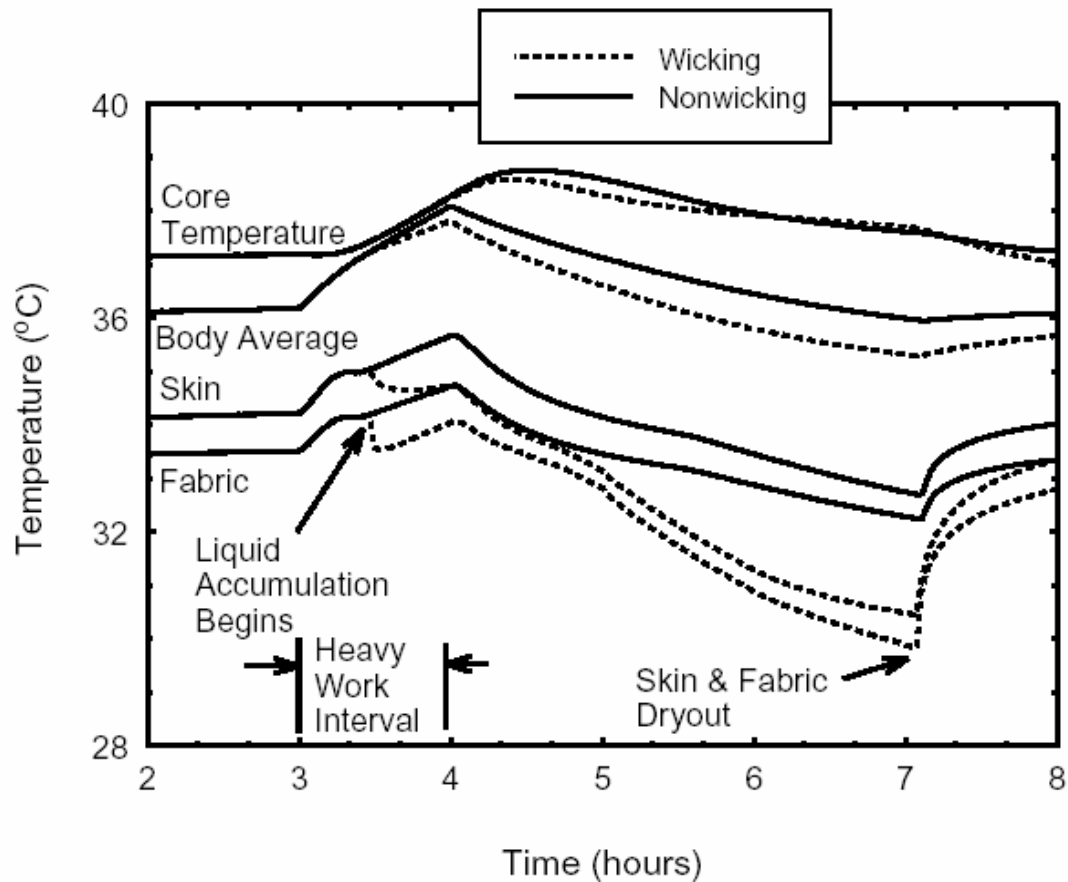
Figure 17. Comparison of a wicking versus a nonwicking fabric (other properties identical) during changes in human work rate [6,7].

The model run in Figure 17 shows that there are some differences in the two fabrics, particularly in the skin temperature and in the fabric temperature. The wicking fabric becomes soggy after a while, as you'd expect, and takes a while to dry out. The nonwicking fabric doesn't soak up water, so the temperatures of the fabric and of the skin remain higher. Perhaps the nonwicking fabric in this case will feel less comfortable. However, the important physiological parameter for heat stress (core temperature) remains equivalent, so this is more a matter of perceptible comfort, rather than differences in heat strain potential between the two fabrics.

Which is more comfortable? I personally prefer to have the liquid sweat wicked away from me, and not to have it running down into my boots. However, I think that the water-repellent treatments are going to be more comfortable over a broader range of conditions, and will perhaps only be less comfortable when the soldier is working and sweating heavily. Even then, I can imagine that I would prefer to have my BDU semi-dry, rather than hanging like a wet rag on me as I try to keep up with everyone else (which I remember all too well from Mountain Warfare School).

## Experiment

A very simple experiment was conducted to see if there are any dramatic differences in the drying behavior of a wetted surface covered by a water-repellent treated fabric. The fabric used in this case was the JLIST ripstop shell fabric (similar to the BDU fabric). One sample was untreated and wicks and absorbs water very quickly. The other sample was treated with a durable water-repellent (DWR) treatment from Nanotex, which is very effective at preventing liquid water from penetrating the fabric. It is important to note that the DWR treatment is applied to both sides of the fabric. It is possible to apply different treatments to the inner and outer fabric surfaces – this would produce results intermediate between the wicking and nonwicking cases.

Fabric Inner Side

Fabric Outer Side

Untreated JSLIST Fabric          Nanotex DWR on JSLIST Fabric
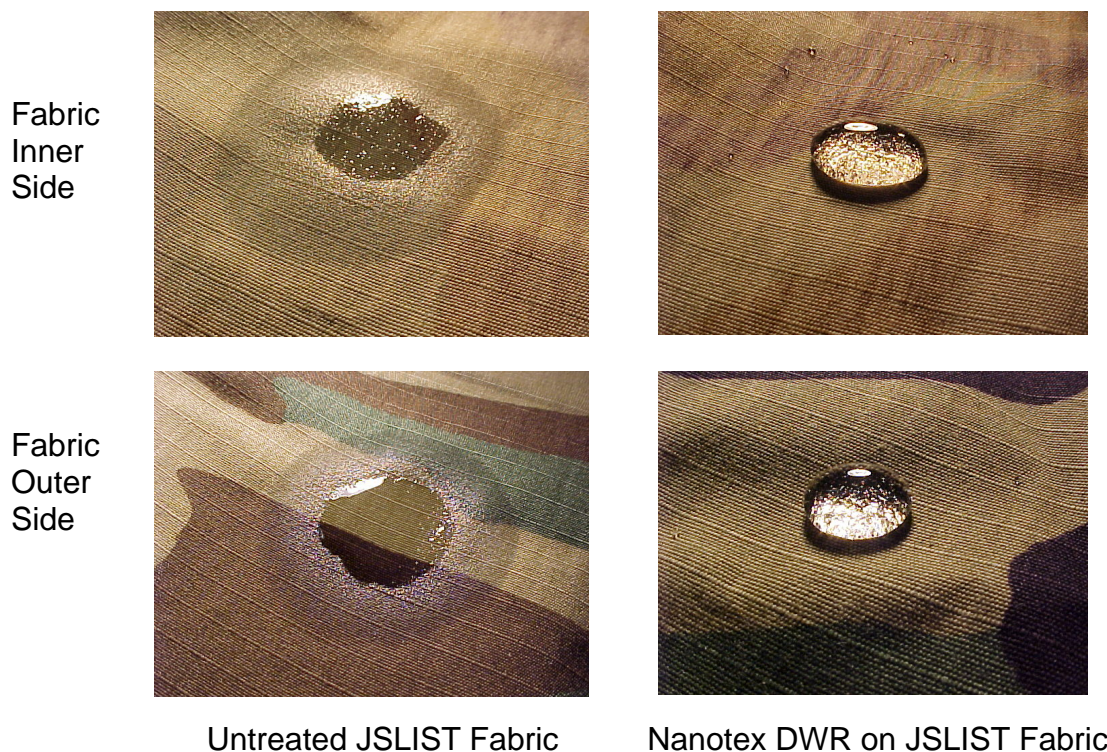
Figure 18. Water droplet on JSLIST fabric (appearance after 20 seconds).

The samples were evaluated in a simple drying experiment to see if there were differences in the drying time for a wetted surface in contact with the fabrics. A piece of paper towel was saturated with liquid water and placed between two layers of the test fabric. The side of fabric that normally contacts the skin was oriented towards the saturated paper towel. The sample was then placed in a test cell that flowed dry gas (0% r.h.) past the two sides of the sample. Two humidity sensors at the outlet of the cell recorded the relative humidity of the exiting gas. As the paper towel dried out, the humidity sensors recorded the drying curve. The rate of fall of the measured relative humidity is related to the drying rate of the fabric system. We assume that a fabric that has a faster drying rate in this test would be more effective at transporting liquid sweat from the skin to the outside environment.
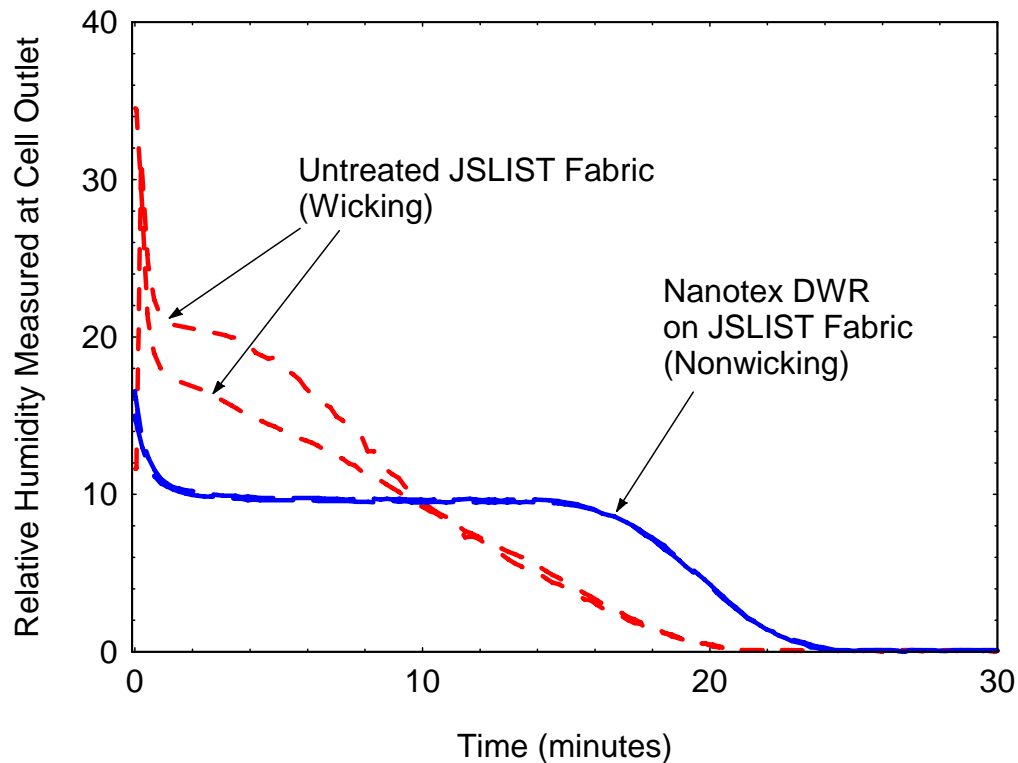
Figure 19.  Relative drying performance of a wicking and a nonwicking fabric.

The wicking case (untreated JSLIST fabric) shows the expected behavior for a wetted fabric.  The interior liquid wicks out through the fabric quickly, and is exposed to the environment, where it can more easily evaporate.  The wicking fabric dries out the interior liquid more quickly, and likely also has a lower surface temperature, due to evaporative cooling, and the lowering of the fabric temperature to the local dewpoint. We have an infrared thermocouple in the system that could look at the fabric surface temperature, if desired, but it wasn't used in this case.  The nonwicking fabric has a very constant drying rate.  The fabric is not wetting out, but is providing some resistance to the diffusion of water vapor through its porous structure.  The falling rate period at the end of the period is when the interior wetted paper towel is starting to dry out completely.

We see some quantitative and qualitative differences in the drying behavior in this simple experiment.  Based on the modeling described above, and on this comparison experiment, we would expect some differences in comfort between DWR-treated and non-treated BDU fabrics for the situation where the soldier is sweating heavily.

*Differential Treatments:*
*Water-Repellent Finish on Outer Fabric Surface,*
*Variable Finish on Inner Fabric Surface*

Five finish variations were supplied for the advanced combat uniform (ACU) fabric. The treatments provided a gradation of wicking properties on the inner fabric face, and various levels of water repellency on the outer fabric face. The addition of wicking properties to a water-repellent fabric should provide more comfort in hot and humid environments. These variable treatments should mitigate the shortcomings of the fabric that was fully treated for water-repellency on both the inner and outer faces

The finish variations examined are show below:

1) Untreated

2) Outer Face: Medium Repellency
   Inner Face: Good Wicking

3) Outer Face: Good Repellency
   Inner Face: Moderate Wicking

4) Good Repellency on
   Both Inner and Outer Face

5) Comparison Reference: Stretch-Woven Nylon Outdoor Clothing Fabric
   (Schoeller Dynamic)
   Good Repellency on Outer Face, Good Wicking on Inner Face

Water drops were applied to either the outer or inner face of fabric (not at the same time). For the inner face, the drop was allowed to spread, and then the wet zone was shown by shining a light through the fabric, as shown in Figure 20.
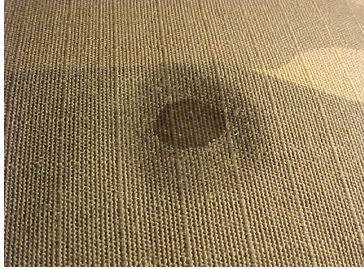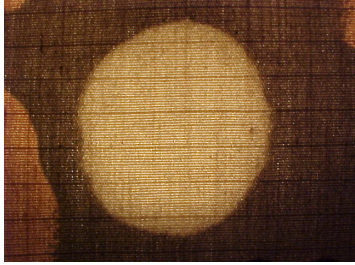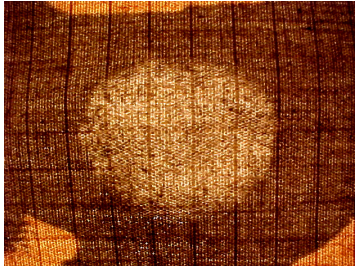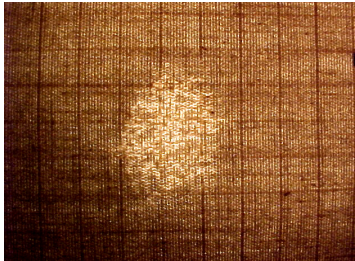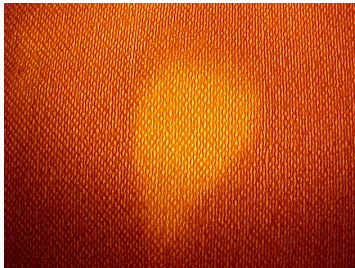
|  | Outer Fabric Face | Backlit Inner Fabric Face |
|---|---|---|
| **1) Untreated Fabric Wicks on Both Sides** | | |
| **2) Moderate Water Repellent on Outer Face, Good Wicking Finish on Inner Face** | | |
| **3) Good Water Repellent on Outer Face, Moderate Wicking Finish on Inner Face** | | |
| **4) Good Water Repellent on Outer and Inner Faces** (backlighting not necessary) | | |
| **5) Stretch Woven Nylon Commercial Outerwear: Good Water Repellent on Outer Face, Good Wicking Finish on Inner Face** | | |

Figure 20.  Water drop on inner/outer faces of fabrics with differential treatments.

In the previous cases, water drops were applied to only the inner or outer fabric face and photographed.

The fabrics that have the differential treatments retain their water repellency on the outer face, even if the inner face has a wicking finish and is wet. As shown in Figure 21, a drop is applied to the inner fabric face and allowed to spread, and then a drop is applied to the outer face. The first picture shows the fabric backlit to show the extent of wicking/spreading on the inner face, and the second picture shows the same fabric with the lighting changed to better show the water droplet on the outer fabric face.

*Treatment (2)*
*Moderate Water Repellent on Outer Face,*
*Good Wicking Finish on Inner Face*
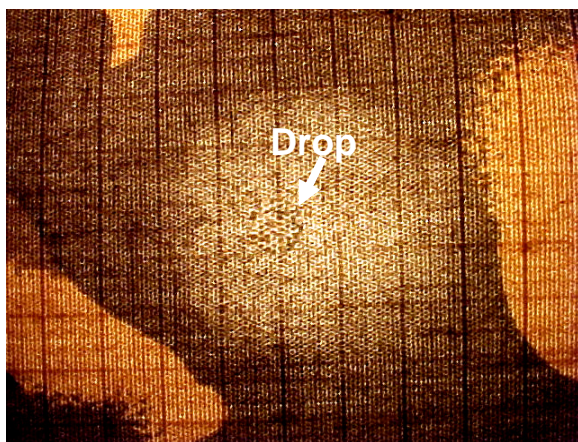


Backlit Outer Face
(difficult to see drop)
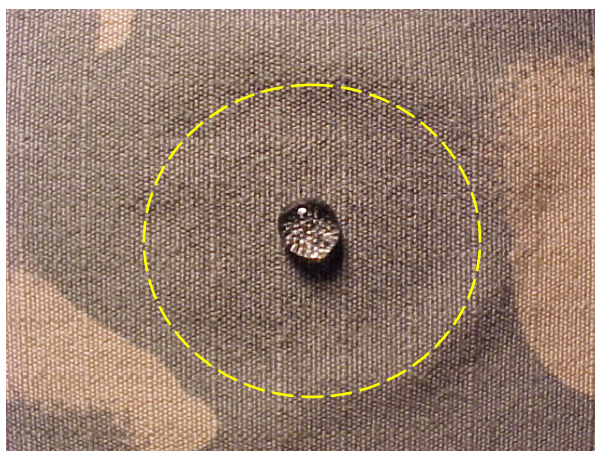
Normal Lighting, Outer Face
(yellow indicates wet area on inside)
(drop rolled slightly to right)

Figure 21. Wet fabric on inside doesn't affect repellency on outside.

*Drying Experiments on Differential DWR Treatments*

Water was applied to the inner surface of the fabrics as shown in Figure 22. The fabric was conditioned in a flow cell, and 0.1 g of water was applied to the surface. Dry air at 30°C flowed past the outer surface of the fabric. A water concentration detector monitored the water vapor concentration of the exiting gas stream. The vapor flux over time was calculated from the gas flow, temperature, and water vapor concentration of the gas stream leaving the test cell.
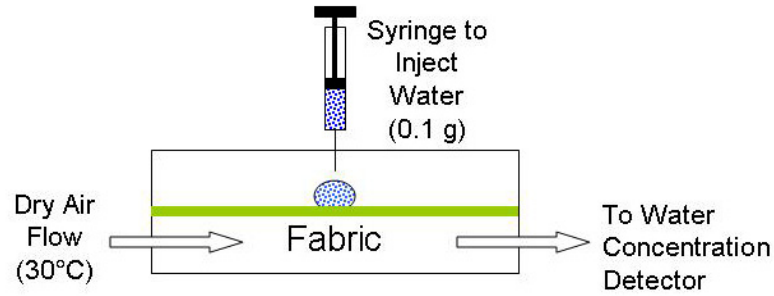
Figure 22.  Test configuration for drying experiments.
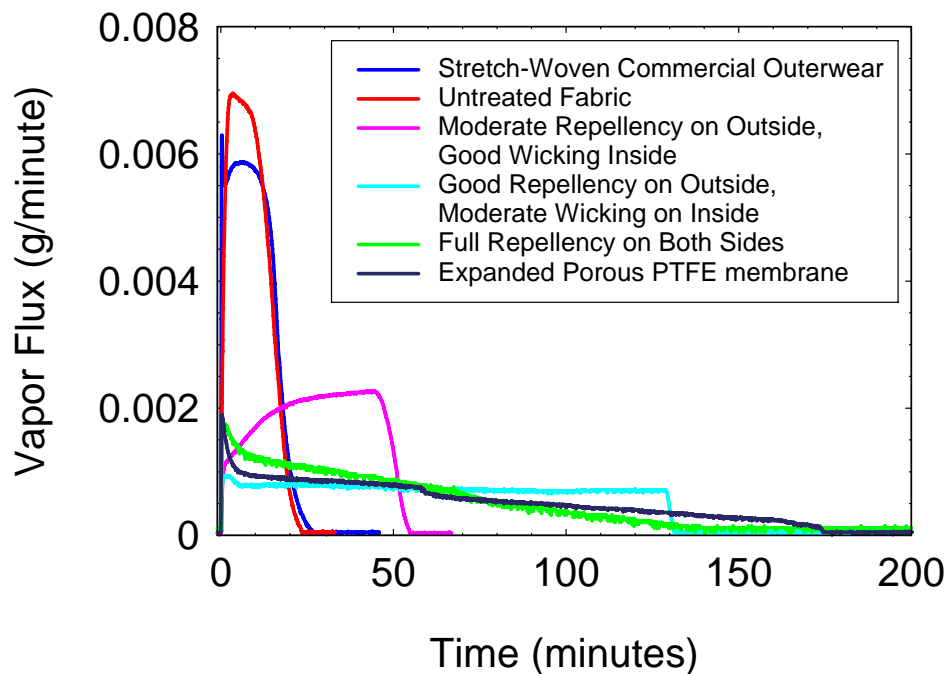


Figure 23.  Drying curves for differential DWR fabric treatments.

The drying time and vapor flux are related to spreading of liquid on the surface and through the fabric thickness. The drying time was hindered by the water repellent finish. The commercial water-repellent "soft-shell" stretch-woven performed as well as the untreated wicking fabric.  The "soft-shell" fabric is specifically engineered to provide good water repellency, while proving comfort through a wicking finish on the inner surface.  The differential treatment on the ACU fabric is not as effective as for the "soft-shell," probably because the ACU fabric is a much heavier material and is a single woven fabric (the "soft-shell" fabric has different fiber configurations on the two sides of the fabric).  The treatment (2) that created an outer face with medium repellency and an inner face with good wicking properties would be comfortable compromise between a fully-repellent fabric and the fully-wicking fabric.

25

## 6. Conclusions

Two of the water-repellent treatments had good durability to laundering.  One treatment had very poor durability, and lost all its water-repellent properties after 20 laundering cycles.  The Quarpel-treated control fabric performed better than any of the experimental treatments.  None of the water-repellent treatments significantly affected the breathability, air flow resistance, or pore size of the BDU fabric.

None of the treatments significantly affected the breathability, air flow resistance, or pore size of the BDU fabric.

It was found that the standard Battle Dress Uniform (BDU) fabric can be modified with very effective water-repellent treatments.  Soldiers' duty and combat uniforms can be made water-resistant and retain the same air permeability and "breathability" properties as the untreated wicking fabric.  Several questions arose as a result of this work.  What are the physiological implications of changing the BDU fabric from a wicking fabric to a non-wicking fabric?  Will the fabric still be comfortable when a soldier is sweating heavily?  Will liquid sweat now remain on the skin underneath the fabric, and is this bad or good?

Following a separate field trial using combat uniforms with and without a DWR treatment, it was found that these treatments decreased the comfort of the uniform in hot environments.  The differences between the comfort of the Control uniform and those treated with the DWR treatments are probably not due to intrinsic differences in the air permeability or the water vapor diffusion resistance (breathability) of the fabric.  It is more likely that the non-wicking behavior of the fabric was responsible for perceived comfort differences, per comments from the field trial, and by analysis of wicking/comfort properties contained in this report.

Some of the DWR treatments are available as coatings on just one side of the fabric.  The outer layer of the fabric can be made water-repellent, while the inner surface retains its wicking characteristics.  Based on comments from the field trial, and modeling results, such asymmetric treatments would improve the comfort of DWR treatments on military duty uniforms as compared to water-repellency on both sides of the fabric.

26

## 7. References

1.  Gibson, P.W., "Effect of Temperature on Water Vapor Transport Through Polymer Membrane Laminates," *Journal of Polymer Testing* **19** (6), 2000.

2.  Gibson, P.W., Rivin, D., Kendrick, C., "Convection/Diffusion Test Method for Porous Textiles," *International Journal of Clothing Science and Technology* **12** (2), 2000.

3.  Gibson, P.W., "Water Vapor Transport and Gas Flow Properties of Textiles, Polymer Membranes, and Fabric Laminates," *Journal of Coated Fabrics* **28**, April, 1999.

4.  Gibson, P.W., Rivin, D., Berezin, A., Nadezhdinskii, A., "Measurement of Water Vapor Diffusion Through Laminated Fabrics and Membranes Using a Diode Laser Spectroscope," *Polymer-Plastics Technology and Engineering* **38** (2), 1999.

5.  United States Patent 6,119,506, September 19, 2000. "Apparatus and method for determining transport properties of porous materials."

6.  Gibson, P.W., "Multiphase Heat and Mass Transfer Through Hygroscopic Porous Media With Applications to Clothing Materials," U.S. Army Natick Research, Development, and Engineering Center Technical Report, Natick/TR-97/005, December, 1996.  DTIC Document online at: http://handle.dtic.mil/100.2/ADA319094

7.  Gibson, P.W., Charmchi, M., "Coupled Heat and Mass Transfer Through Hygroscopic Porous Materials -- Application to Clothing Layers," *Journal of the Society of Fiber Science and Technology, Japan (Sen-i Gakkaish*i) **53** (5), May, 1997.

8.  Gibson, P.W., Kendrick, C., Rivin, D., "Convection/Diffusion Test Method for Porous Materials Using the Dynamic Moisture Permeation Cell," U.S. Army Natick Research, Development, and Engineering Center Technical Report, Natick/TR-97/014, April, 1998.

9. International Organization for Standardization, ISO 11092:1993, Standard Test Method: Textiles -- Physiological effects -- Measurement of thermal and water-vapour resistance under steady-state conditions (sweating guarded-hotplate test), Technical Committee TC 38, Textiles, 1993.

10. American Society for Testing and Materials (ASTM) E96 Standard Test Methods for Water Vapor Transmission of Materials.

**This page intentionally left blank**

**Appendix A**

SUMMARY OF CONVECTION/DIFFUSION TEST METHOD

**Appendix A**

**Summary of Convection/Diffusion Test Method**

This test method is explained in the technical report "Convection/Diffusion Test Method for Porous Materials Using the Dynamic Moisture Permeation Cell" [8]. This test method measures water vapor diffusion resistance and air permeability (resistance to air flow) from the same test. A cartoon of the test setup is shown below -- more details from the report. In this test method we systematically change the pressure drop across the sample to obtain different air flow through the fabric. If you have an air-impermeable fabric is not air permeable, there is no air flow, and the results don't change, but if the fabric is air-permeable, there are large differences between various fabrics. Since there is a humidity difference across the sample, the water vapor diffusion properties are also obtained from this test. At the condition of 0 pressure drop, a water vapor diffusion resistance property is measured that correlates with properties measured via the sweating guarded hot plate (ISO 11092) [9] or the ASTM E96 methods [10].
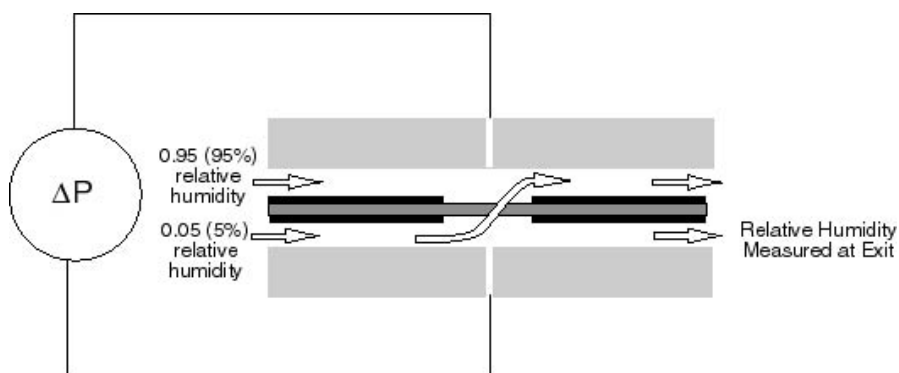


Figure A-1. Schematic of convection/diffusion test. Air can flow across the fabric in either direction depending on the particular pressure drop set by the computer.

Test Conditions – Water Vapor Diffusion/Convection

Temperature = 30 $^\circ$C
Sample Area = 10 cm²

Flow Rates on top and bottom = 2000 cm$^3$/minute
Humidity on Top = .95 (95%); Humidity on Bottom =.05 (5%)
Pressure drop varied in increments between approximately –150 to 150 Pa.
Note: Humidity of 1.0 = 100%; 0.5 inches of water is about 125 Pa.

To convert from flow resistance in units of 1/m to air permeability as used in the textile industry (m³/s-m², or ft³/min-ft²), where the pressure drop is usually 0.5 inches of water:

$Q_{metric}$(m³/s-m²) = $\Delta p / R\mu$

$\Delta p$ = pressure drop in Pa (N/m²); Frazier air permeability uses 125 Pa (0.5 inches of $H_2O$)

$R$ = air flow resistance (1/m) ; value obtained from DMPC measurement

$\mu$ = air viscosity (17.85 x $10^{-6}$ kg/m-s at 20°C)

$Q_{english}$ (ft³/min-ft²) = 197 $Q_{metric}$
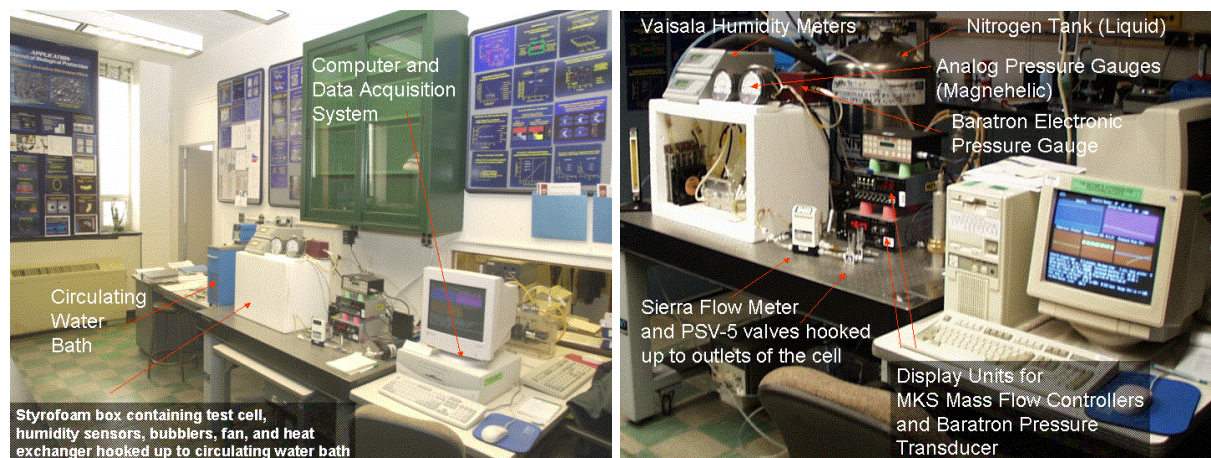


**Dynamic Moisture Permeation Cell (DMPC)**
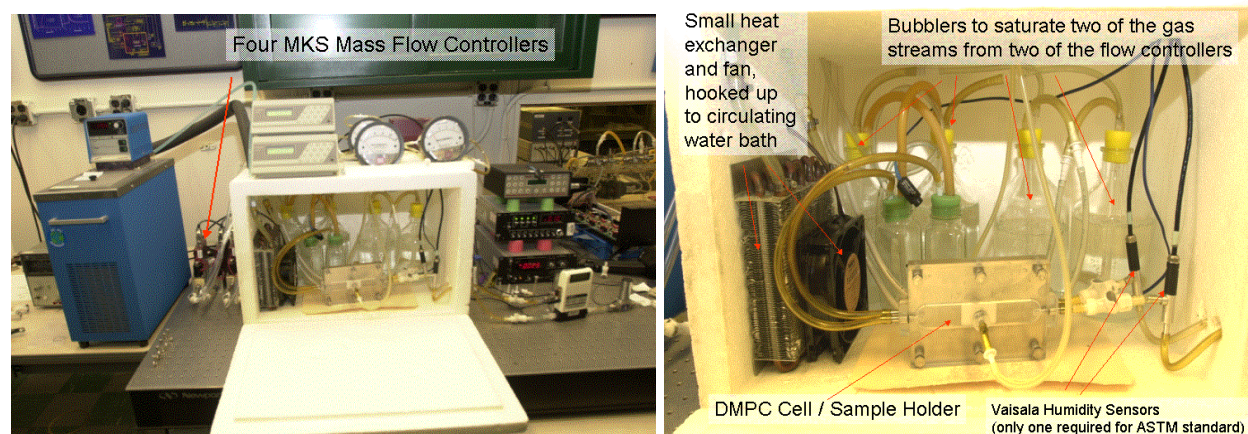


**Conditioning Chamber and Sample Holder**

Figure A-2. Components of the Dynamic Moisture Permeation Cell (DMPC).

Figure 22 and 23 give typical water vapor diffusion properties of commercially available protective clothing materials to give a basis of comparison for the fabrics tested in this report.


**"Breathability" Comparison of Commercial Outerwear Shell Layers**
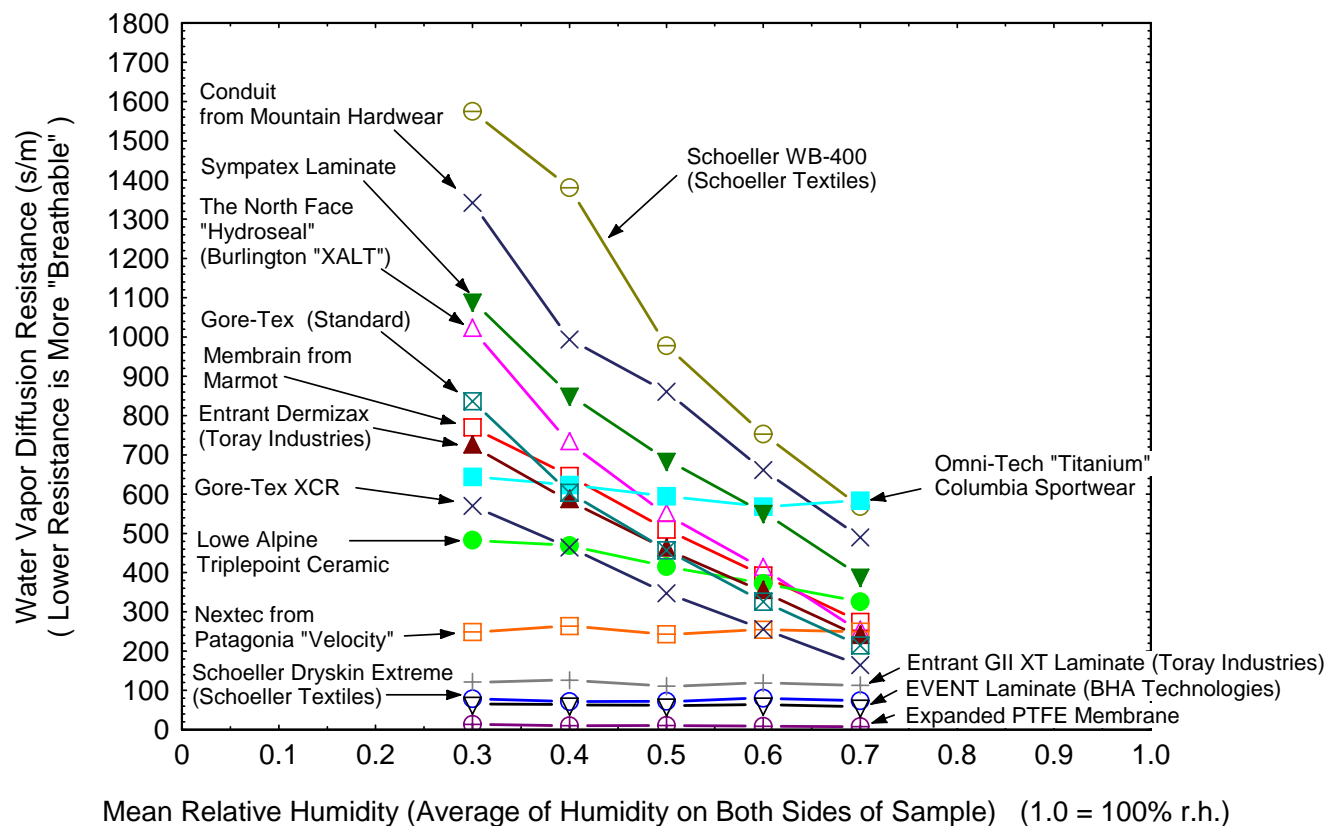


Figure A-3. Water vapor diffusion resistance of a variety of commercial waterproof/breathable membrane laminates.
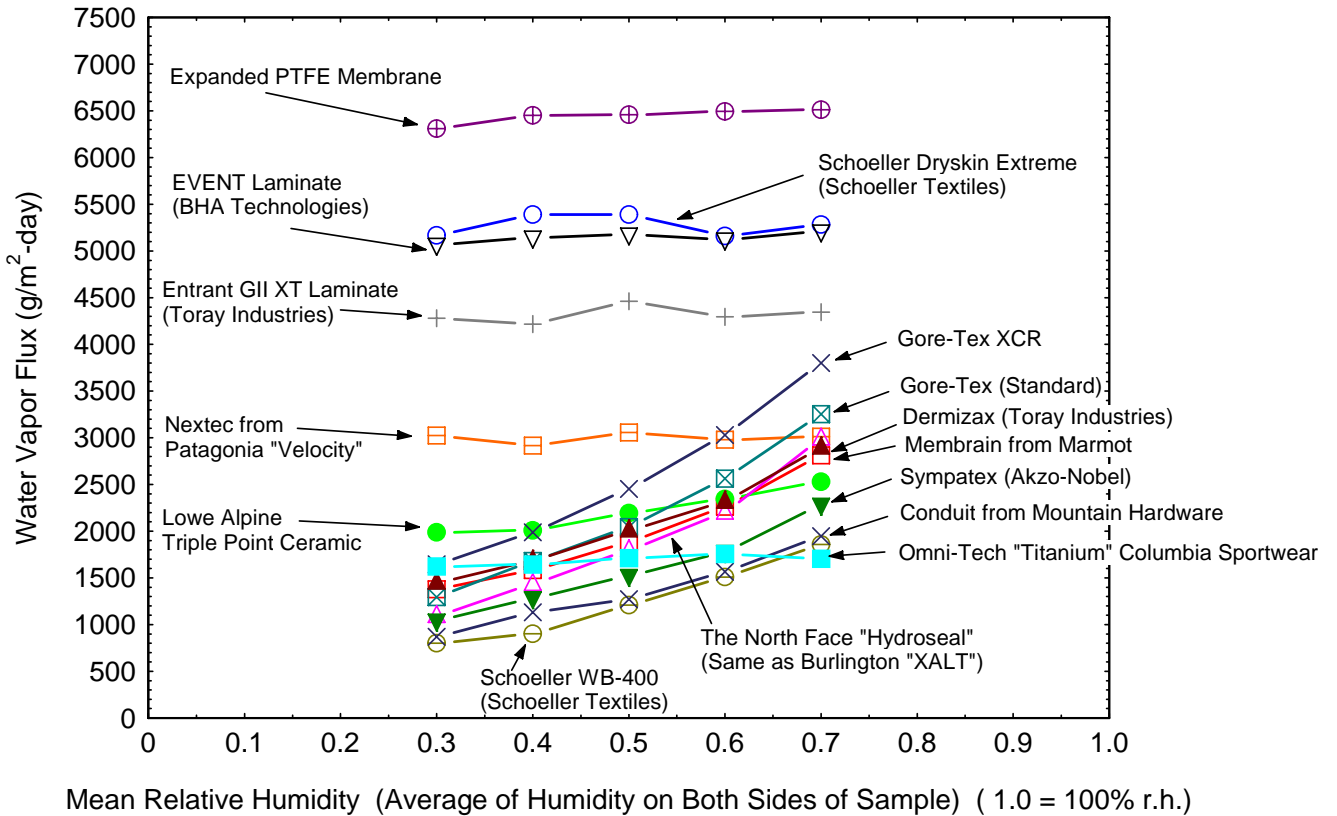
Figure A-4. Typical water vapor flux measurements for a variety of commercial waterproof/breathable membrane laminates.

**Water Vapor Pure Diffusion Test Summary - Dynamic Moisture Permeation Cell**

In this test method, air at two different relative humidities flows over the two sides of the test sample.  By measuring the water vapor concentration at the exits of the cell, it is possible to measure how much water vapor crosses the sample.  Results may be shown in terms of water vapor flux (grams/square meter/day) or resistance to the diffusion of water vapor (units of s/m).  The resistance units make comparing results obtained at different environmental conditions much easier.  The lower the diffusion resistance, the more water vapor gets through the material.  The reason for doing the testing this way is that some materials like Gore-Tex, Sympatex, etc., have much better water vapor transport properties when they are in a humid environment than when they are in a dry environment, relatively speaking.  Other materials, such as most textiles or microporous membranes, have a nearly constant water vapor diffusion resistance regardless of the environmental conditions

Test Conditions – Water Vapor Diffusion
Temperature = 30°C
Gas Flow Rate = 2000 cm³/minute, countercurrent flow
Sample Size = .0025 m² (25 cm²)

Note:  relative humidity of 100% is 1.0, so 0.50 is 50% r.h., etc.

| Setpoint # | Humidity on Top of Sample | Humidity on Bottom of Sample | Mean Relative Humidity | Humidity Gradient |
|---|---|---|---|---|
| 1 | 0.55 | 0.05 | 0.30 | 0.50 |
| 2 | 0.65 | 0.15 | 0.40 | 0.50 |
| 3 | 0.75 | 0.25 | 0.50 | 0.50 |
| 4 | 0.85 | 0.35 | 0.60 | 0.50 |
| 5 | 0.95 | 0.45 | 0.70 | 0.50 |

**Appendix B**


**COUPLED HEAT AND MASS TRANSFER THROUGH HYGROSCOPIC POROUS MATERIALS:  APPLICATION TO CLOTHING LAYERS**

## Appendix B

## Coupled Heat and Mass Transfer Through Hygroscopic Porous Materials: Application to Clothing Layers

### INTEGRATION OF A HUMAN THERMAL PHYSIOLOGY CONTROL MODEL WITH A NUMERICAL MODEL FOR COUPLED HEAT AND MASS TRANSFER THROUGH HYGROSCOPIC POROUS TEXTILES

**P.W. Gibson and M. Charmchi***

U.S. Army Natick Research, Development and Engineering Center
Natick, Massachusetts

*University of Massachusetts Lowell
Lowell, Massachusetts

### ABSTRACT

A comprehensive numerical model developed for the coupled transport of energy and mass through porous hygroscopic materials was integrated with an existing human thermal physiology model to provide appropriate boundary conditions for the clothing model. The human thermal control model provides skin temperature, core temperature, skin heat flux, and water vapor flux, along with liquid water accumulation at the skin surface. The integrated model couples the dynamic behavior of the clothing system to the human physiology of heat regulation. This model provided the opportunity to systematically examine a number of clothing parameters, which are traditionally not included in steady-state thermal physiology studies, and to determine their potential importance under various conditions of human work rates and environmental conditions.

### NOMENCLATURE

$c_a$    water vapor concentration of ambient atmosphere [kg/m$^3$]

$c_p$    constant pressure heat capacity [J/kg·K]

$(c_p)_{ds}$    constant pressure heat capacity of the dry solid [J/(kg·K)]

$(c_p)_w$    constant pressure heat capacity of liquid water [4182 J/(kg·K) @290 K]

$(c_p)_v$    constant pressure heat capacity of water vapor [1862 J/(kg·K) @290 K]

$(c_p)_a$    constant pressure heat capacity of dry air [1003 J/(kg·K) @290 K]

$C_p$    mass fraction weighted average constant pressure heat capacity [J/kg·K]

$c_{so}$    water vapor concentration at skin surface [kg/m$^3$]

$d_f$    effective fiber diameter [m]

$D_a$    diffusion coefficient of water vapor in air [m$^2$/s]

$D_{eff}$    effective gas phase diffusivity [m$^2$/sec]

$D_{solid}$    effective solid phase diffusion coefficient [m$^2$/s]

$E$    metabolic energy generated in muscle layer due to exercise [W/m$^3$-s]

$\delta f$    fabric thickness [m]

$h_c$    convective heat transfer coefficient [W/m$^2$-s]

$h_m$    convective mass transfer coefficient [m/s]

$\Delta h_{vap}$    enthalpy of vaporization per unit mass [J/kg]

$k$    thermal conductivity [J/s·m·K]

| $k_\beta$ | thermal conductivity of body tissue [J/(s·m·K)] |
|---|---|
| $k_{s0}$ | reference body tissue thermal conductivity [0.498 J/(s·m·K)] |
| $k_{ds}$ | thermal conductivity of the dry solid [J/(s·m·K)] |
| $k_w$ | thermal conductivity of liquid water [0.600 J/(s·m·K) @290 K] |
| $k_v$ | thermal conductivity of saturated water vapor [0.0246 J/(s·m·K) @380K] |
| $k_a$ | thermal conductivity of dry air [0.02563 J/(s·m·K) @290 K] |
| $k_\varepsilon$ | $\partial \langle P_c \rangle / \partial \varepsilon_\beta$ [N/m²] |
| $K$ | permeability coefficient [m²] |
| $K_\beta$ | Darcy permeability for liquid phase [m²] |
| $L$ | total half-thickness of body model system [0.056 m] |
| $\dot{m}$ | mass flux of water vapor across the sample [kg/s] |
| $M_a$ | molecular weight of air [28.97 kg/kgmole] |
| $M_w$ | molecular weight of water vapor [18.015 kg/kgmole] |
| $M_{avl}$ | liquid water available on skin surface for evaporation [kg/m²] |
| $p$ | pressure [N/m²] |
| $p_\gamma$ | total gas pressure [N/m²] |
| $p_a$ | partial pressure of air [N/m²] |
| $p_v$ | partial pressure of water vapor [N/m²] |
| $p_s$ | saturation vapor pressure (function of T only) [N/m²] |
| $P_c$ | $p_\gamma$-$p_\beta$, capillary pressure [N/m²] |
| $q_m$ | rate of heat generation due to metabolism [W/m³-s] |
| $Q$ | volumetric flow rate [m³/s] |
| $Q_l$ | enthalpy of desorption from solid phase to liquid phase per unit mass [J/kg] |
| $\check{q}$ | heat flux vector [J/s·m²] |
| $\Delta Q_{sh}$ | metabolic energy generated due to shivering [W/m³·s] |
| $R$ | universal gas constant [8314.5 N·m/(kg·K)] |
| $R_f$ | textile measurement (@$\phi$=0.65), grams of water absorbed per 100 grams of fiber [fraction] |
| $R_{skin}$ | equilibrium regain at fiber surface [fraction] |
| $R_{total}$ | total fiber regain from last time step [fraction] |
| $R_{bl}$ | diffusion resistance of boundary air layers [s/m] |
| $s$ | sweating rate [kg/m²·s] |
| $s_0$ | reference basal sweating rate [2.80 x10⁶ kg/m²·s] |
| $S$ | saturation, fraction of void space occupied by liquid [fraction] |
| $s_{ir}$ | irreducible saturation; saturation level at which liquid phase is discontinuous |
| $T$ | temperature [K] |
| $T_a$ | ambient air temperature [K] |
| $T_\beta$ | average body temperature [K] |
| $T_{sk}$ | skin temperature [K] |
| $\Delta T_\beta$ | deviation from the body's setpoint [K] |
| $t$ | time [s] |
| $\langle v_\beta^V \rangle$ | volume average liquid velocity [m/s] |

*Greek Letters*

| | |
|---|---|
| $\alpha_{k1}$ | thermal proportional control coefficient [1/K] |
| $\alpha_{k2}$ | thermal proportional control coefficient [1/K] |
| $\alpha_{sh1}$ | shivering proportional control coefficient [W/m³·K] |
| $\alpha_{sh2}$ | shivering proportional control coefficient [W/m³·K²] |
| $\alpha_{sh3}$ | shivering proportional control coefficient [W/m³·K] |
| $\alpha_{s1}$ | sweating proportional control coefficient [kg/m²·s·K] |
| $\alpha_{s2}$ | sweating proportional control coefficient [kg/m²·s·K⁴] |
| $\varepsilon_\sigma(t)$ | volume fraction of the solid phase |
| $\varepsilon_\beta(t)$ | volume fraction of the liquid phase |
| $\varepsilon_\gamma(t)$ | volume fraction of the gas phase |
| $\varepsilon_{ds}$ | volume fraction of the dry solid (constant) |
| $\varepsilon_{bw}(t)$ | volume fraction of the water dissolved in the solid phase |
| $\phi$ | $p_v/p_s$, relative humidity |
| $\gamma$ | thermal rate control coefficient [s/K] |
| $\mu_\beta$ | viscosity of the liquid phase [for water, 9.8 x 10⁻⁴ kg/m·sec at 20°C] |
| $\rho$ | density [kg/m³] |
| $\rho_\beta$ | density of liquid phase [kg/m³] |
| $\rho_{ds}$ | density of dry solid [for polymers typically 900 to 1300 kg/m³] |
| $\rho_w$ | density of liquid water [approximately 1000 kg/m³] |
| $\rho_\gamma$ | density of gas phase (mixture of air and water vapor) [kg/m³] |
| $\rho_v$ | density of water vapor in the gas volume (equivalent to mass concentration) [kg/m³] |
| $\rho_a$ | density of the inert air component in the gas volume (equivalent to mass of air/total gas volume) [kg/m³] |
| $\tau$ | tortuosity factor |
| $\xi$ | dummy integration variable |

*Subscripts*

| | |
|---|---|
| $\sigma$ | designates a property of the solid phase |
| $\beta$ | designates a property of the liquid phase |
| $\gamma$ | designates a property of the gas phase |

3

38

## INTRODUCTION

Many models for human heat stress and thermal comfort assume that clothing has a constant heat and mass transfer resistance. Such models do not account for the very large changes in clothing properties which often occur under non-steady-state conditions. Neglecting factors such as liquid water wicking, the heat released and stored when water is absorbed/desorbed into textile fibers, and the changes in fabric porosity due to fiber swelling/shrinkage, leads to significant errors when accounting for the energy and mass transfer between the human body and the ambient environment. Even under steady-state conditions, many properties which we treat as constant for modeling purposes can change by an order of magnitude depending upon the actual use conditions. This uncertainty about material properties becomes much greater under the unsteady boundary conditions which are the norm in actual clothing systems, where a steady-state condition is rarely achieved.

The intent of this study is to develop and demonstrate the use of an integrated model which is capable of including many of the nonlinear and transient properties of hygroscopic textiles in the analysis of the interactions between human thermal physiology and clothing systems.

## HUMAN THERMAL MODEL

We selected a particularly simple human thermal physiology model to integrate with the clothing model. The model includes appropriate control functions for variables such as sweating rate, metabolic activity, blood flow effects, etc. The model is one-dimensional in nature and treats the body as a single thermal zone. In effect, to put it indelicately, the model behaves like a living sweaty slab of tissue that responds to the environment in a manner similar to the way the human body responds. We would expect that the next step is to integrate the clothing model with more sophisticated multi-zone human thermal models (Stolwijk and Hardy, 1977; Wissler, 1985), in a manner similar to that done by Jones (1992).

The body is modeled as a one-dimensional slab (Crosbie et al., 1963; Shitzer and Chato, 1985). The thermal conductivity of the body is a function of the average body temperature. Blood flow effects are included in the effective thermal conductivity for the tissue. The body is divided into three layers. The core layer generates basal metabolic energy. The muscle layer generates energy due to exercise, or due to shivering. The skin layer produces no heat, but generates sweat at rates specified by the physiological control functions. The body is assumed symmetrical so that the computational domain extends from the body center of symmetry outward to the skin. A schematic of the body model, including clothing layers, is shown in Figure 1.

4

39
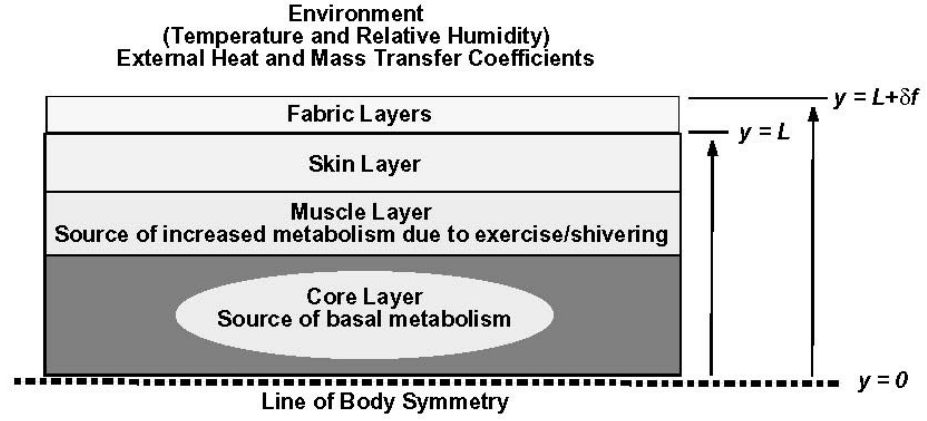
Figure 1. One-dimensional thermoregulatory model of the human body, including clothing layers.

The governing equations for the thermal physiology model are given below:

*Energy Equation*

$$\rho_B c_{p_B} \frac{\partial T}{\partial t} = k_B \frac{\partial^2 T}{\partial y^2} + q_m \tag{1}$$

*Initial conditions:*

at $t=0$:  $T=T(y)$ (2)

*Boundary Conditions:*

at $y=0$:  $\quad \frac{\partial T}{\partial y} = 0$ (3)

at $y=L$:  $\quad -k_B \frac{\partial T}{\partial y} = m\Delta h_{vap} + h_c (T_{sk} - T_a)$ (4)

Average body temperature is defined as:

$$T_B = \frac{1}{L} \int_0^L T(\xi,t)\, d\xi \tag{5}$$

40

The deviation from the body's setpoint is defined as:

$$\Delta T_B = T_B - 35.75\ ^\circ C = T_B - 308.9\ K \tag{6}$$

The body's thermal conductivity, which varies to simulate vasodilation effects, is defined in terms of a reference thermal conductivity, and proportional and rate control functions which kick in when the average body temperature deviates from the setpoint (defined as 35.75 °C).

For temperatures above the body's setpoint:

$$k_B = k_{B0}\left(1 + \alpha_{k1}\Delta T_B + \gamma\frac{dT_B}{dt}\right) \leq 1.511 k_{B0} \qquad \Delta T_B > 0 \tag{7}$$

For temperatures below the body's setpoint:

$$k_B = k_{B0}\left(1 + \alpha_{k2}\Delta T_B + \gamma\frac{dT_B}{dt}\right) \geq 0.675 k_{B0} \qquad \Delta T_B < 0 \tag{8}$$

The sweating rate from the skin is also defined in terms of deviations from body setpoint; for temperatures above the setpoint, the sweating rate is given by:

$$s = s_0 + \alpha_{s1}\Delta T_B + \alpha_{s2}\left(\Delta T_B\right)^4 \leq 60 s \qquad \Delta T_B > 0 \tag{9}$$

For temperatures below setpoint, the sweating rate is given by the basal rate:

$$s = s_0 \qquad \Delta T_B < 0 \tag{10}$$

For no clothing layer, with a given mass transfer coefficient, mass flux of water vapor from the skin surface is given by:

$$\dot{m} = \begin{cases} h_m\left(c_{sk} - c_a\right) & M_{avl} > 0 \\ \text{minimum of } \left[s, h_m\left(c_{sk} - c_a\right)\right] & M_{avl} = 0 \end{cases} \tag{11}$$

When a clothing layer covers the skin surface, the mass transfer coefficient is replaced by the effective diffusion coefficient of the fabric or air space combined with the thickness of the first control volume above the skin surface.

The mass of liquid water available at the skin surface $\left(M_{avl}\right)$ is given by:

$$M_{avl} = M_{avl}|_{t=0} + \int_0^t \left[s(\xi) - \dot{m}(\xi)\right]d\xi \tag{12}$$

41

Metabolic heat generation is distributed between the various layers:

--No heat generation occurs in the outer skin layer.
--Basal metabolic heat generation takes place in the core layer:

$$(q_m = 1339 \ \mathrm{W/m^3}).$$

The muscle layer produces heat due to exercise, or due to shivering:

$$q_m = E \qquad\qquad \Delta T_B > 0 \tag{13}$$

$$q_m = E + \Delta Q_{sh} \qquad \Delta T_B < 0 \tag{14}$$

$$\Delta Q_{sh} = -\alpha_{sh1}\Delta T_B + \alpha_{sh2}\left(\Delta T_B\right)^2 \qquad -1 \le \Delta T_B < 0 \tag{15}$$

$$\Delta Q_{sh} = 660.3\left(\mathrm{W/m^3}\right) - \alpha_{sh2}\Delta T_B \qquad \Delta T_B < -1 \tag{16}$$

## CLOTHING MODEL

The clothing model is based on volume-averaging techniques (Whitaker, 1977), which are used to develop a model for coupled heat and mass transfer through hygroscopic porous materials (Gibson, 1994). This model is similar to others developed to account for diffusion properties of textile-based materials (Farnworth, 1986; Wehner et al., 1988; Jones et al., 1990; Li et al., 1992; Tao et al., 1993; Le and Ly, 1995). The boundary conditions for the fabric's external surface use heat and mass transfer coefficients. The boundary conditions for the fabric's inner surface are determined by the vapor flux and heat flux from the human thermal control model.

For most of these simulations, we are only looking at the coupled diffusion of heat and water vapor. If there is any extra liquid sweat which builds up on the skin surface, it does not drip off or wick into the fabric. Later in this paper we discuss a simulation which uses a very simple way of including liquid sweat wicking. We are also ignoring gas convection due to pressure differences, which can arise either due to body movement, or due to external air movement (wind).

For one-dimensional transient diffusion, the major simplifying assumptions are: 1) there is no liquid or gas phase convection, 2) there is no liquid phase present, 3) the transport is one-dimensional ($y$-direction). The variables given below have been volume-averaged according to the relations given by Gibson (1994).

*Governing Differential Equations for Clothing Model:*

*Energy equation:*

$$\rho C_p \frac{\partial T}{\partial t} + \left(Q_l + \Delta h_{vap}\right)\dot{m}_{sv} = \frac{\partial}{\partial y}\left(k_{eff}\frac{\partial T}{\partial y}\right) \tag{17}$$

7

42

*Solid phase continuity equation:*

$$\rho_w \frac{\partial}{\partial t}\left(\varepsilon_{bw}\right) + \dot{m}_{sv} = 0 \quad \text{or} \quad \frac{\partial}{\partial t}\left(\varepsilon_{bw}\right) + \frac{\dot{m}_{sv}}{\rho_w} = 0$$

(18)

*Gas phase diffusion equation:*

$$\frac{\partial}{\partial t}\left(\varepsilon_\gamma \rho_v\right) - \dot{m}_{sv} = \frac{\partial}{\partial y}\left(\mathcal{D}_{eff}\frac{\partial \rho_v}{\partial y}\right)$$

(19)

*Volume fraction constraint:*

$$\varepsilon_\gamma + \varepsilon_{bw} + \varepsilon_{ds} = 1$$

(20)

*Thermodynamic relations*

$$p_a = p_\gamma - p_v$$

$$p_a = \rho_a \frac{R}{M_a} T$$

$$p_v = \rho_v \frac{R}{M_w} T$$

(21-23)

*Sorption Relation* (Lotens, 1993 )

$$\varepsilon_{bw} = 0.578 R_f \left(\varepsilon_{ds}\frac{\rho_{ds}}{\rho_w}\right)(\phi)\left[\frac{1}{(0.321+\phi)} + \frac{1}{(1.262-\phi)}\right]$$

(24)

The source term due to vapor sorption is modeled by assuming that diffusion into the fiber is quasi-steady state (Le and Ly, 1995). The polymer at the fiber's surface is assumed to immediately come into equilibrium with the relative humidity of the gas phase within the control volume for that grid point. The mass flux into or out of the fiber is calculated by:

$$\dot{m}_{sv} = \frac{D_{solid}\rho_{ds}}{d_f^{\,2}}\left(R_{total} - R_{skin}\right)$$

(25)

*Transport Coefficients and Mixture Properties*

$$\rho = \varepsilon_{bw}\rho_w + \varepsilon_{ds}\rho_{ds} + \varepsilon_\gamma\left(\rho_v + \rho_a\right)$$

(26)

$$C_p = \frac{\varepsilon_{bw}\rho_w\left(c_p\right)_w + \varepsilon_{ds}\rho_{ds}\left(c_p\right)_{ds} + \varepsilon_\gamma\left[\rho_v\left(c_p\right)_v + \rho_a\left(c_p\right)_a\right]}{\rho}$$

(27)

8

43

For fabrics with significant porosity, an expression for the effective thermal conductivity is given by (Kerner, 1956; Progelhof, 1976):

$$k_{eff} = k_{\gamma} \left\{ \frac{\left[1 + (\varepsilon_{bw} + \varepsilon_{ds})\right] k_{\sigma} + \varepsilon_{\gamma} k_{\gamma}}{\varepsilon_{\gamma} k_{\sigma} + \left[1 + (\varepsilon_{bw} + \varepsilon_{ds})\right] k_{\gamma}} \right\} \tag{28}$$

$$k_{\gamma} = \left( \frac{k_v \rho_v + k_a \rho_a}{\rho_v + \rho_a} \right) ; \quad k_{\sigma} = \left( \frac{k_w \rho_w \varepsilon_{bw} + k_{ds} \rho_{ds} \varepsilon_{ds}}{\rho_w \varepsilon_{bw} + \rho_{ds} \varepsilon_{ds}} \right) \tag{29-30}$$

$$\mathcal{D}_{eff} = \frac{\mathcal{D}_a \varepsilon_{\gamma}}{\tau} \tag{31}$$

$$\mathcal{D}_a \ (\mathrm{m^2 \cdot s^{-1}}) = 2.23 \times 10^{-5} \left( \frac{T}{273.15} \right)^{1.75} \tag{32}$$

$$Q_l \ (\mathrm{J/kg}) = 1.95 \times 10^5 (1 - \phi) \left( \frac{1}{(0.2 + \phi)} + \frac{1}{(1.05 - \phi)} \right) \tag{33}$$

$$\Delta h_{vap} \ (\mathrm{J/kg}) = 2.792 \times 10^6 - 160 T - 3.43 T^2 \tag{34}$$

$$p_s \ (\mathrm{N \cdot m^{-2}}) = 614.3 \exp\left\{ 17.06 \left[ \frac{(T - 273.15)}{(T - 40.25)} \right] \right\} \tag{35}$$

**Initial and Boundary Conditions**

*Boundary Conditions ($\delta f$ refers to fabric thickness):*

$$h_c (T_\infty - T)_{y = L + \delta f} = -k_{eff} \frac{\partial T}{\partial x} \bigg]_{y = L + \delta f} \tag{36}$$

$$h_m (\rho_{v\infty} - \rho_v)_{y = L + \delta f} = -D_{eff} \frac{\partial \rho_v}{\partial x} \bigg]_{y = L + \delta f} \tag{37}$$

*Initial Conditions:*

$$T(x, t = 0) = T_0$$
$$\rho_v(x, t = 0) = \phi_0 p_s (@T_0)$$
$$\varepsilon_{bw}(x, t = 0) = \varepsilon_{bw0}$$

9

44

The material properties used for the numerical simulations are given in Table 1, and are similar to those for a typical cotton fabric.

**Table 1. Assumed Fabric Layer Properties**

Thickness $\delta f$:  9.14 x $10^{-4}$ m
Apparent Bulk Density (Dry): 438 kg/$m^3$
Regain at 65% relative humidity $R_f$ : 0.06
Effective Diffusivity $D_{eff}$ :  6.09 x$10^{-6}$  $m^2$/s
Fabric Tortuosity $\tau$ :  2.9
Effective solid phase diffusion coefficient $D_{solid}$ :  4.0 x$10^{-14}$  $m^2$/sec
Effective fiber diameter $d_f$: 3.6 x$10^{-6}$  m
Density of dry polymer $\rho_{ds}$ : 1500 kg/$m^3$
Heat capacity of dry polymer $(c_p)_{ds}$ : 1200 J/kg-K
Thermal conductivity of dry polymer $k_{ds}$ : 0.16 J/sec-m-K

## EFFECT OF CHANGES IN ENVIRONMENTAL RELATIVE HUMIDITY

We first examine the performance of the integrated model for the situation where the environmental relative humidity is changed, while the environmental temperature remains constant.  This situation is chosen to illustrate the difference between a hygroscopic fabric, which actively absorbs water vapor and releases the heat of sorption, and a nonhygroscopic fabric, which remains passive.

We examine two cases for the clothing model.  One case is a highly hygroscopic fabric which has a high heat of sorption (Table 1).  The second case is to take the exact same fabric properties, except to let the regain equal zero at all conditions, which turns the fabric into a nonhygroscopic fabric such as polyester.  The nonhygroscopic fabric has all the other properties of the hygroscopic fabric, such as thermal conductivity, heat capacity, thickness, effective diffusivity, etc., but it will not absorb water vapor from the atmosphere.

We start off by letting the human thermal model, with the clothing layer, equilibrate for 3 hours under warm and dry conditions of 35°C and 10% relative humidity.  The human work rate is kept constant at 50 Watt/$m^2$, which corresponds to a fairly light work rate.  To observe the differences between the two fabrics we  suddenly change the relative humidity to 90% for 1 hour, beginning at hour 3, and then change the relative humidity back to 10%, at hour 4.

By doing this, we can get a feel for how much skin temperature (which relates to comfort) would be affected by the different regain properties of a hygroscopic versus a nonhygroscopic fabric.  In this case we are only looking at environmental changes.  We will get some of the same effects if the environmental conditions remain the same, and if we change the metabolic energy generation rate due to exercise, which will change the sweating rate, which will also show up in the heat generated/absorbed in the hygroscopic clothing layer.

Two cases are shown in Figure 2 for a hygroscopic and a nonhygroscopic fabric: for a human work rate of 50 Watt/m$^2$, and an environmental temperature of 35°C, the relative humidity was changed from 10% to 90% for one hour.



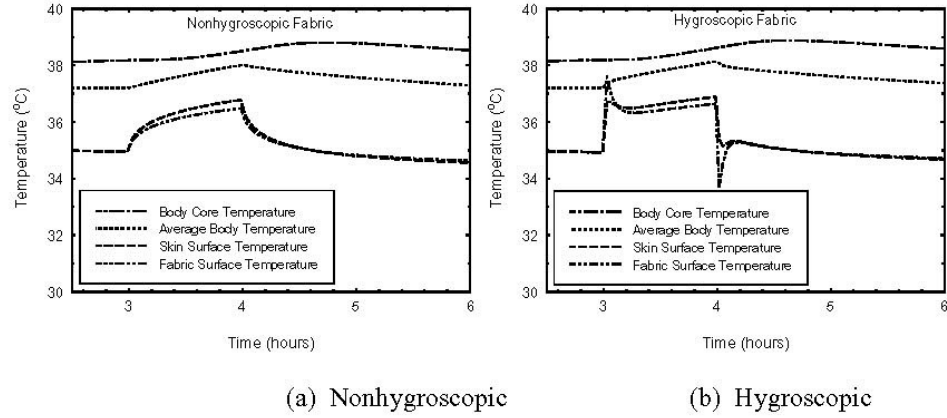(a) Nonhygroscopic          (b) Hygroscopic

Figure 2. Calculated temperatures for nonhygroscopic and hygroscopic fabrics covering sweating human, when subjected to large changes in environmental relative humidity.

The large differences in skin temperature profiles seen in Figure 2 imply differences in perceived comfort of these two fabrics. For the thin fabrics used in this simulation, we see very little difference between the two fabrics for the overall thermal balance, as reflected by the nearly identical body core temperatures for the two situations. We would expect that some of these short-term transient effects, which affect comfort, surface temperature, etc., would be much less important to the overall steady-state heat transfer.

Figure 2 shows that we can get changes in fabric surface temperature just due to changes in environment. Most standard human thermal models which only use steady-state clothing properties, would not pick up changes such as these. These are surface temperature differences between the two cases of several °C, which can be detected by infrared sensors, so it is possible that the ability to model the surface temperatures of clothing in this way would be useful in the study of the thermal signature of clothed humans.

Besides the temperature variables shown in Figure 2, the integrated model gives explicit values for a great many other variables, such as sweating rate, humidities, vaporization rate, porosity changes, percent water absorbed as a function of location in the clothing system, etc. In Figures 3 and 4, we may observe a comparison of the hygroscopic versus nonhygroscopic case for the three quantities of skin relative humidity, liquid sweat accumulation at the skin surface, and volumetric vaporization rate at the skin surface. The volumetric vaporization rate is equal to the vaporization rate per unit skin area divided by the thickness of the first control volume at the skin surface.

Figure 3.  Skin surface relative humidity, liquid sweat accumulation at skin surface, and vaporization rate at skin surface, for hygroscopic fabric case.


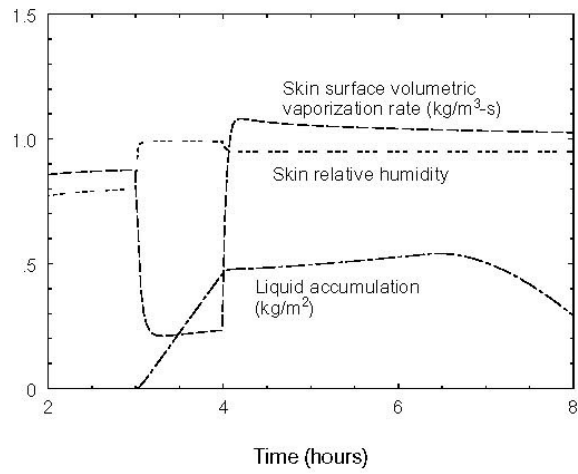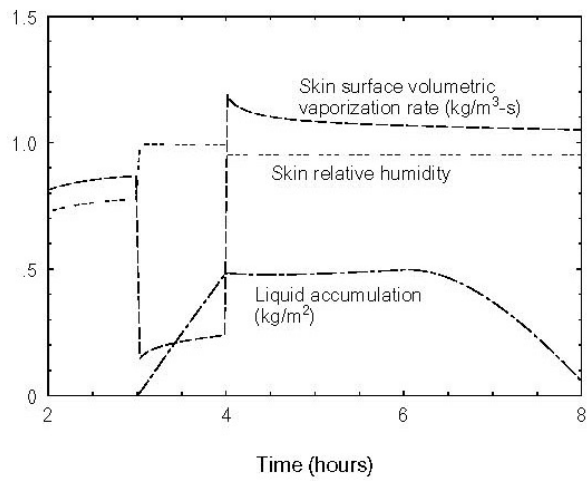
Figure 4.  Skin surface relative humidity, liquid sweat accumulation at skin surface, and vaporization rate at skin surface, for nonhygroscopic fabric case.

## EFFECT OF ORDER OF CLOTHING LAYERS

Keeping in mind the extreme simplicity of the assumptions incorporated into our single-zone human thermal physiology model, we can immediately start to use the integrated model to look at factors such as the arrangement and properties of fabric layers, and how they might affect how a fabric system performs. One particularly easy thing to try is to vary the arrangement of two fabric layers on the body. Such questions about system design often come up in cold weather clothing and chemical protective clothing systems, where we may know the total thermal or water vapor resistance of the clothing system, but we also have options about the order of arrangement of those layers.

We will place the two fabric layers on the body model, and only vary the hygroscopic nature of each fabric layer. We again examine the case where the relative humidity is changed from 10% to 90% relative humidity for one hour at hour 3, and then back to 10% relative humidity at hour 4. The four cases examined are listed below:

Case I -- both layers nonhygroscopic
Case II -- outer layer hygroscopic, inner layer nonhygroscopic
Case III -- inner layer hygroscopic, outer layer nonhygroscopic
Case IV -- both layers hygroscopic

Cases I and IV were shown previously in Figure 2, if we assume that the total thickness of those fabrics were equal to that of two layers. In Figure 5 we show the calculated fabric surface temperatures, for each of the four cases, and in Figure 6 we show the calculated skin surface temperatures.
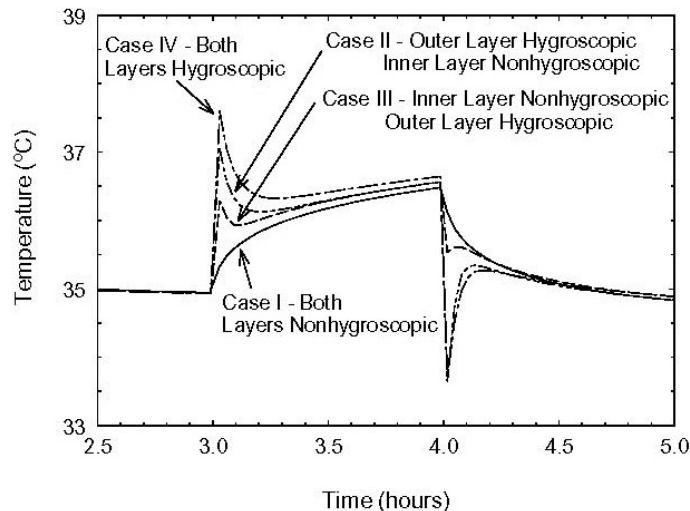
Figure 5. Calculated fabric surface temperatures, for four layering arrangements.
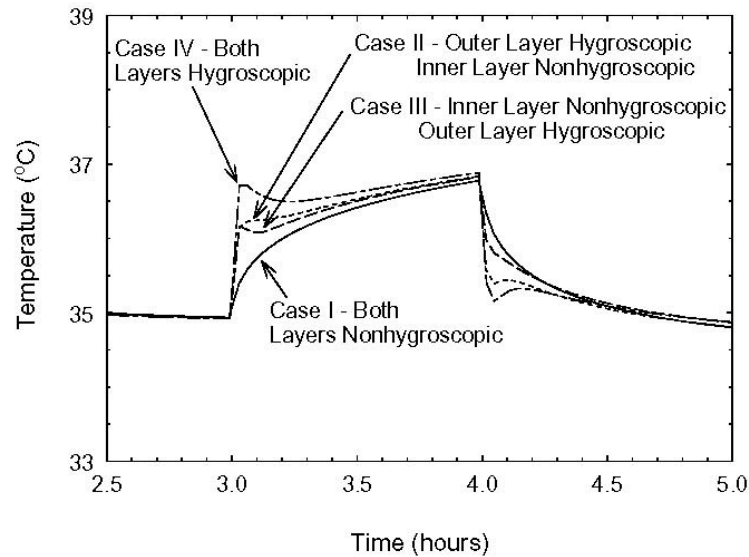


Figure 6. Calculated skin surface temperatures, for four layering arrangements.

We can see a steady progression of relative differences in the fabric surface temperature and skin temperature due to the differences in fabric regain and the arrangement of the two layers, but again we didn't see much difference in core temperature, which means these differences have the most impact on perceived comfort, rather than overall heat stress. We also emphasize again that we are not letting liquid sweat wick into the clothing layers, but only allow it to build up in a layer on the skin surface.

**EFFECT OF CHANGES IN HUMAN WORK RATE**

We can also use the combined model to look at how hygroscopic clothing properties interact with increases in sweating rate and exercise levels due to changes in human work rate, while the environmental factors remain constant.

The first situation we examine is a change in human work rate from 20 W/m² (light work) to 100 W/m² (fairly heavy work). The environmental conditions are 30°C, 65% r.h. We again examine the difference between clothing layers which differ only in their hygroscopic nature. No air layers are present, and again the fabric does not wick liquid sweat, so we are only looking at the diffusion of heat and water vapor. Human work rate is changed to the higher level between hours 3 and 4.

14

49
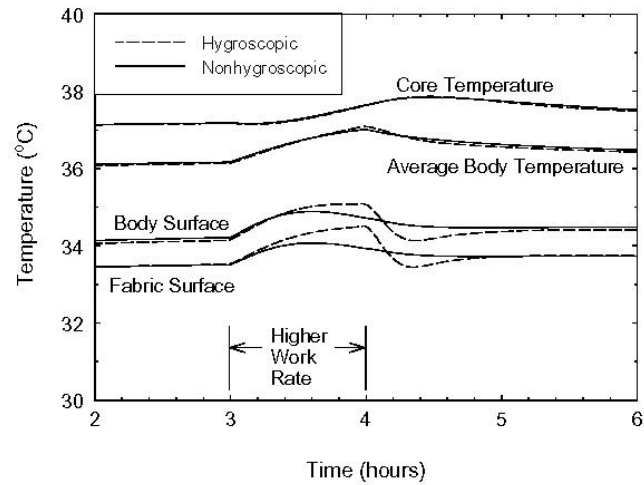
Figure 7. Differences in calculated temperatures between hygroscopic and nonhygroscopic fabrics, for a change in work rate from 20 to 100 W/m².
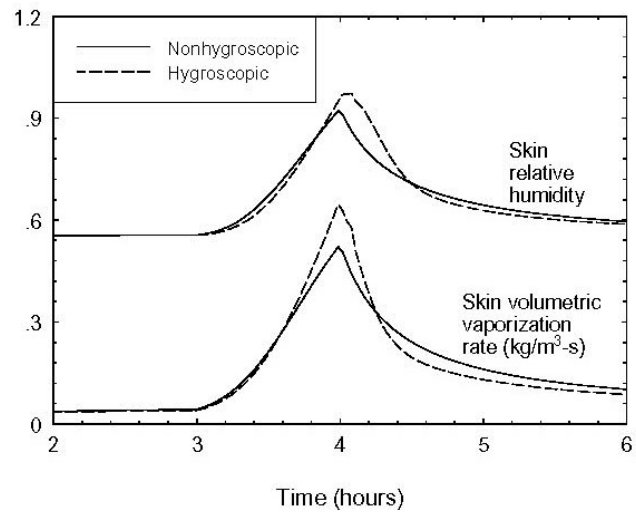


Figure 8. Differences in vaporization rate and skin relative humidity for hygroscopic and nonhygroscopic fabrics, for a change in work rate from 20 to 100 W/m².

Figure 7 and 8 show some of the same effects of fiber hygroscopicity that we saw for the change in environmental conditions, but in this case, they are influenced by the increases in vapor concentration caused by increased sweating and vaporization rates at the skin surface.

50

Up to this point, we have neglected sweat accumulation within the clothing layers, which is quite ludicrous for most normal fabric materials. The large amount of sweat generated by the body would certainly be absorbed by the clothing, which would produce much higher vaporization rates than those predicted by the pure diffusion model. Fortunately it is quite easy to incorporate simple wicking effects into the clothing model, which is covered in the next section.

## A SIMPLE MODEL OF WICKING EFFECTS IN CLOTHING

To incorporate liquid sweat movement and accumulation in clothing layers, we must modify the one-dimensional governing equations to include the liquid phase (Gibson, 1994). The major simplifying assumptions are that we again neglect gas phase convective transport, and only consider one dimension. The major change is that we may now have the liquid phase present within the averaging control volume, and we must keep track of the liquid volume fraction, and the rate of liquid-to-vapor phase change in the control volume. The modified set of governing equations are:

*Energy equation:*

$$\rho C_p \frac{\partial T}{\partial t} + \left[ \rho_\beta \left( c_p \right)_\beta \left\langle \overset{\text{v}}{v}_\beta \right\rangle \right] \frac{\partial T}{\partial y} + \Delta h_{vap} \dot{m}_{lv} + \left( Q_l + \Delta h_{vap} \right) \dot{m}_{sv} = \frac{\partial}{\partial y} \left( k_{eff} \frac{\partial T}{\partial y} \right) \tag{36}$$

*Solid phase continuity equation:*

$$\rho_\beta \frac{\partial}{\partial t} \left( \varepsilon_{bw} \right) + \dot{m}_{sv} = 0 \quad \text{or} \quad \frac{\partial}{\partial t} \left( \varepsilon_{bw} \right) + \frac{\dot{m}_{sv}}{\rho_\beta} = 0 \tag{37}$$

*Gas phase diffusion equation:*

$$\frac{\partial}{\partial t} \left( \varepsilon_\gamma \rho_v \right) - \dot{m}_{lv} - \dot{m}_{sv} = \frac{\partial}{\partial y} \left( \mathcal{D}_{eff} \frac{\partial \rho_v}{\partial y} \right) \tag{38}$$

*Liquid phase continuity equation:*

$$\frac{\partial \varepsilon_\beta}{\partial t} + \frac{\partial \left\langle \overset{\text{v}}{v}_\beta \right\rangle}{\partial y} + \frac{\dot{m}_{lv}}{\rho_\beta} = 0 \quad \text{or} \quad \frac{\partial \varepsilon_\beta}{\partial t} = - \frac{\partial \left\langle \overset{\text{v}}{v}_\beta \right\rangle}{\partial y} - \frac{\dot{m}_{lv}}{\rho_\beta} \tag{39}$$

*Liquid phase equation of motion:*

$$\left\langle \overset{\text{v}}{v}_\beta \right\rangle = - \left( \frac{K_\beta}{\mu_\beta} \right) \nabla \left[ \left( p_a + p_v \right) - P_c \right] \tag{40}$$

*Volume fraction constraint:*

$$\varepsilon_\gamma + \varepsilon_\beta + \varepsilon_{bw} + \varepsilon_{ds} = 1 \tag{41}$$

16

51

The thermodynamic relations remain the same as equations (21-23), and the sorption relation and source term due to vapor sorption remain the same as equations (24) and (25) respectively.

In a similar manner, we determine a source term for evaporation or condensation from the liquid phase to gas phase by assuming that if there is any liquid phase present, the partial vapor pressure is saturated. If the vapor pressure is above saturation, then condensation takes place until the partial vapor pressure is at saturation.

*Transport Coefficients and Mixture Properties*

The transport coefficients and mixture properties are of the same form as were given previously, but must be modified to include the liquid phase volume fraction.

$$k_{eff} = k_\gamma \left\{ \frac{\left[1 + \left(\varepsilon_\beta + \varepsilon_{bw} + \varepsilon_{ds}\right)\right]k_\sigma + \varepsilon_\gamma k_\gamma}{\varepsilon_\gamma k_\sigma + \left[1 + \left(\varepsilon_\beta + \varepsilon_{bw} + \varepsilon_{ds}\right)\right]k_\gamma} \right\} \tag{42}$$

$$k_\sigma = \left( \frac{k_w \rho_\beta \varepsilon_\beta + k_w \rho_\beta \varepsilon_{bw} + k_{ds} \rho_{ds} \varepsilon_{ds}}{\rho_\beta \varepsilon_\beta + \rho_\beta \varepsilon_{bw} + \rho_{ds} \varepsilon_{ds}} \right)$$

$$k_\gamma = \left( \frac{k_v \rho_v + k_a \rho_a}{\rho_v + \rho_a} \right) \tag{43-44}$$

$$\mathcal{D}_{eff} = \frac{\mathcal{D}_a \varepsilon_\gamma}{\tau} \tag{45}$$

$$\rho = \varepsilon_\beta \rho_\beta + \varepsilon_{bw} \rho_\beta + \varepsilon_{ds} \rho_{ds} + \varepsilon_\gamma \left(\rho_v + \rho_a\right) \tag{46}$$

$$C_p = \frac{\varepsilon_\beta \rho_\beta \left(c_p\right)_\beta + \varepsilon_{bw} \rho_\beta \left(c_p\right)_\beta + \varepsilon_{ds} \rho_{ds} \left(c_p\right)_{ds} + \varepsilon_\gamma \left[\rho_v \left(c_p\right)_v + \rho_a \left(c_p\right)_a\right]}{\rho} \tag{47}$$

The set of equations (36-47) given above are of a form compatible with those often used by people modeling moisture migration or drying processes in porous material. There are several simplifying assumptions we can make which will allow us to proceed to a very simple model of wicking effects in clothing, but first we may discuss factors relating to capillary pressure and liquid phase permeability in clothing materials.

17

52

Capillary pressure $P_c$ is often a function of the fraction of the void space occupied by the liquid. Liquid present in a porous material may be either in a pendular state, or in a continuous state. If the liquid is in a pendular state, it is in discrete drops or regions which are unconnected to other regions of liquid. If liquid is in the pendular state, there is no liquid flow, since the liquid does not form a continuous phase. There may be significant capillary pressure present, but until the volume fraction of liquid rises to a critical level to form a continuous phase, there will be no liquid flow. This implies that there is a critical saturation level, which we can think of a the relative proportion of liquid volume within the gas phase volume, which must be reached before liquid movement may begin.

Experimentally measured liquid capillary curves often show significant hysteresis depending on whether liquid is advancing (imbibition) or receding (drainage) through the porous material. A typical curve is shown below in Figure 9.
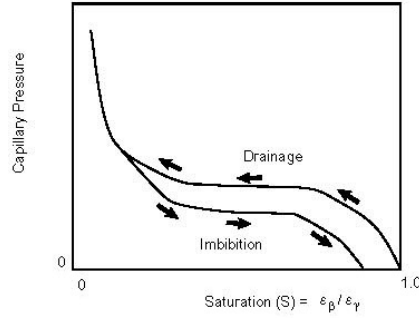


Figure 9. Typical appearance of capillary pressure curves as a function of liquid saturation for porous materials.

We may take a definition for liquid saturation as:

$$S = \frac{V_\beta}{V_\gamma + V_\beta} = \frac{\varepsilon_\beta}{\varepsilon_\beta + \varepsilon_\gamma} \tag{48}$$

The point at which the liquid phase becomes discontinuous is often called the irreducible saturation ($s_{ir}$) (Kaviany, 1991). When the irreducible saturation is reached, the flow is discontinuous, which implies that liquid flow ceases when:

$$\varepsilon_\beta < s_{ir}\left[1 - \left(\varepsilon_{ds} + \varepsilon_{bw}\right)\right] \tag{49}$$

An empirical equation given by Stanish et al. (1986), suggests a form for the equation for capillary pressure as a function of fraction of void space occupied by liquid:

$$P_c = a\left(\frac{\varepsilon_\beta}{\varepsilon_\gamma}\right)^{-b} \text{, where } a \text{ and } b \text{ are empirical constants} \tag{50}$$

18

53

For liquid permeability as a function of saturation (Stanish et al., 1986):

$$K_\beta = \begin{cases} 0; & \left(\varepsilon_\beta / \varepsilon_\gamma\right) < s_{ir} \\ K_\beta^s \left\{ 1 - \cos\left[ \frac{\pi}{2} \frac{\left(\varepsilon_\beta / \varepsilon_\gamma\right) - s_{ir}}{\left(1 - s_{ir}\right)} \right] \right\}; & \left(\varepsilon_\beta / \varepsilon_\gamma\right) \geq s_{ir} \end{cases} \tag{51}$$

where $K_\beta^s$ is the liquid phase Darcy permeability when fully saturated.

Equations (50) and (51) can be incorporated in a straightforward manner into the one-dimensional model; however, the technical problem of measuring the empirical constants contained in these equation is considerable.

Another way to look at a moisture diffusivity equation is to consider the moisture distribution throughout the porous material as akin to a diffusion process. By combining the conservation of mass and Darcy's equation, a differential equation for the local saturation $S$ may be written as (Chatterjee, 1985):

$$\frac{\partial S}{\partial t} = \frac{\partial}{\partial y}\left[ F(s) \frac{\partial S}{\partial y} \right] \tag{52}$$

where the "moisture diffusivity" is given by:

$$F(s) = \frac{\left(\dfrac{K_\beta}{\mu_\beta}\right)\left(\dfrac{dP_c}{dS}\right)}{\left(\varepsilon_\beta + \varepsilon_\gamma\right)} \tag{53}$$

If we rewrite the saturation variable $S$ in terms of its original definition:

$$S = \frac{V_\beta}{V_\gamma + V_\beta} = \frac{\varepsilon_\beta}{\varepsilon_\beta + \varepsilon_\gamma} \quad ;$$

the differential equation for liquid migration under the influence of capillary pressure may be written as:

$$\frac{\partial}{\partial t}\left( \frac{\varepsilon_\beta}{\left(\varepsilon_\beta + \varepsilon_\gamma\right)} \right) = \frac{\partial}{\partial y}\left[ \frac{\left(\dfrac{K_\beta}{\mu_\beta}\right)\left(\dfrac{dP_c}{dS}\right)}{\left(\varepsilon_\beta + \varepsilon_\gamma\right)} \frac{\partial}{\partial y}\left( \frac{\varepsilon_\beta}{\left(\varepsilon_\beta + \varepsilon_\gamma\right)} \right) \right] \tag{54}$$

19

54

Although we have available the form of these relations for the capillary pressures, and permeability as a function of saturation and irreducible saturation, we have very little data available on the actual values of permeabilities for representative textile fabrics. Wicking studies on fabrics are usually carried out parallel to the plane of the fabric by cutting a strip, dipping one end in water, and studying liquid motion as it wicks up the strip (Ghali et al., 1994, Ghali et al., 1995). However, wicking from the body through the fabric layer takes place perpendicular to the plane of the fabric, where the transport properties are quite different due to the highly anisotropic properties of woven fabrics.

The usefulness of the relations contained in equations (48-54) are that they allow one to model the drying behavior of porous materials by accounting for both a constant drying rate period and a falling rate period. In the constant rate drying period, evaporation takes place at the surface of the porous material, and capillary forces bring the liquid to the surface. When irreducible saturation is reached in regions of the porous solid, drying becomes limited by the necessity for diffusion to take place through the porous structure of the material, which is responsible for the "falling rate" period of drying. These effects are most important for materials which are thick, or of low porosity. For materials of the porosity and thickness typical of woven fabrics, almost all drying processes are in the constant rate regime, which suggests that many of the complicating factors which are important for thicker materials can be safely ignored. Studies on the drying rates of fabrics (Crow, 1987; Crow and Osczevski, 1993; Crow and Dewar, 1993) suggest that simply assuming drying times proportional to the original liquid water content are a good predictor of the drying behavior of both hygroscopic and nonhygroscopic fabrics. Wicking processes perpendicular to the plane of the fabric take place very quickly, and the falling rate period is very short once most of the liquid has evaporated from the interior portions of fabrics. The one-dimensional modeling we have done of fabric drying also suggests that this is true: for thin fabrics, the drying rate is constant for most of the drying time, and the falling rate period is very short. We have also found that extremely small time steps must be taken computationally to capture the falling rate period.

For these reasons, we decided that it may not be productive at this point to include numerical values for the empirical factors and constants contained in equations (48-54) in the integrated clothing/human thermal physiology model. However, it is a very simple matter to assume a very high liquid permeability and very high capillary pressures, which cause any liquid sweat remaining at the skin surface to instantly be distributed within the free porosity of the fabric. This allows us to look at two different clothing materials which are identical in all their properties except that one material will wick sweat away from the skin surface, while the other does not allow wicking through its structure. When liquid is present, wicking effects quickly overwhelm any of the other diffusive effects, both due to the evaporation of liquid water within the clothing, and the increase in thermal conductivity of the porous matrix due to the liquid water which builds up within the clothing layers. An example is shown in figure 10 for the case of a wicking versus a nonwicking fabric, when a human goes from a light work rate (20 Watt/m$^2$) to a heavy work rate (200 Watt/m$^2$) for 1 hour, and then back to a light work rate. Environmental conditions in both cases are air temperature of 30°C and relative humidity of 65%.
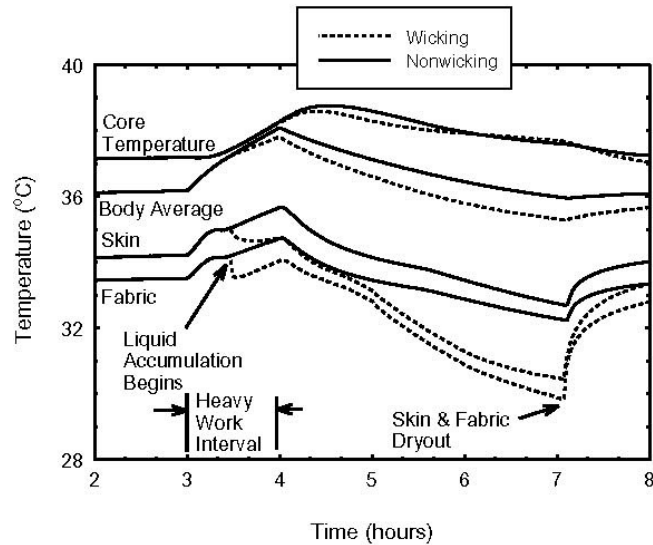
Figure 10. Comparison of a wicking versus a nonwicking fabric (other properties identical) during changes in human work rate.

**CONCLUSIONS**

The integration of a model of the human thermal control system with a material model for the coupled diffusion of mass and energy through hygroscopic porous materials has made it possible to examine phenomena such as transient changes in skin and clothing surface temperature as influenced by the hygroscopicity of fabric layers. Factors important to the design of clothing systems, such as the placement and order of fabric layers, and the relative important of wicking versus nonwicking fabrics, may be assessed with this simple model.

The clothing model and the physiological model are relatively independent. This should make it possible to incorporate the clothing model into more realistic multi-zone models of the human thermophysiological control system.

**REFERENCES**

Crosbie, R., Hardy, J., Fessenden, E., 1963, Electrical Analog Simulation of Temperature Regulation in Man. In *Temperature: Its Measurement and Control in Science and Industry, Volume 3, Part 3, Biology and Medicine*, Hardy, J. ed., Herzfeld, C., editor-in-chief, Reinhold Publishing Corporation, New York, pp. 627-635.

Crow, R., Moisture, 1987, Liquid and Textiles -- A Critical Review, Defense Research Establishment Ottowa, DREO Report No. 970, June 1987.

21

56

Crow, R., Osczevski, R.,
Times, Defense Research Estab

Crow, R., Dewar, M., 199
Defense Research Establishmer

Farnworth, B., 1986, A n
vapour through clothing, *Textil*

Ghali, K., Jones, B., Trad
International Journal of Heat ar

Gahli, K., Jones, B., Trad
Thermal and Fluid Science 9, p

Gibson, P.W., 1994, Gov
Hygroscopic Porous Media witl
TR-95/004, U.S. Army Natick l

Jones, B. W., 1992, Tran
environment, *ASHRAE Transac*
Chatterjee, P., 1985, *Absorbenc*

Jones, B., Ito, M., McCul
system," *Proceedings of the Int*
Texas, October, pp. 66-67, 199(

Kaviany, M., 1991, *Princ*
York, pp. 428-431.

Kerner, E., 1956, The ele
*Physical Society*, B69, p. 802.

Le, C., Ly, N., 1995, Hea
of Wool, Cotton, Nylon, and Pc
212.

Li, Y., Holcombe, B.V.,
moisture and heat in wool fabri

Lotens, W., 1993, *Heat T*
published by TNO Institute for

Progelhof, R., Throne, J.,
conductivity of composite syste
615-625.

Shitzer, A., Chato, C., 19
*Transfer in Medicine and Biolo*
and Eberhart, R.C.), Plenum Pr

Stolwijk, J., Hardy, J., 19
*Section 9*, edited by S. Geiger,

Stanish, M., Schajer, G.,
Hygroscopic Porous Media, *AI*

Tao, Y., Besant, R., Rezk
*International Journal of Heat a*

Wehner, J., Miller, B., R
fabric barriers, *Textile Researcl*

Whitaker, S., 1977, A Th
Academic Press, New York.

Wissler, E., 1985, Mathe
models. In *Heat and Mass Tra*
Eberhart, R.C.), Plenum Press,